

# Bioengineered Skin in Psoriasis Modeling

Investigation of Automated Injection Molding of Dermo-Epidermal Models as compared with Benchmark Manual Fabrication.

Maria Sarkiri  
4633423



# Bioengineered Skin in Psoriasis Modeling

Investigation of Automated Injection Molding of  
Dermo-Epidermal Models as compared with Benchmark  
Manual Fabrication

by

Maria Sarkiri

to obtain the degree of Master of Science in Biomedical Engineering  
(track: Biomaterials & Tissue Biomechanics)  
at the Delft University of Technology,  
to be defended publicly on Monday October 22, 2018 at 12:00 PM.

Student number: 4633423  
Thesis committee: Prof. dr. ir. A. Zadpoor, Exam Committee Chair  
Dr. ir. L. Fratila Apachitei, TU Delft, supervisor  
Dr. ir. E. Carroll  
Dr. ir. V. Popovich  
ETH supervisors: Prof. dr. ir. M. Meboldt  
S. Fox

An electronic version of this thesis is available at <http://repository.tudelft.nl/>.



# Abstract

Bioengineered skin was initially developed for clinical application in reconstructive surgery, but nowadays it is also considered as a suitable skin model for research. Research applications range from assessment of cosmetic and pharmaceutical products to the modeling of pathological skin conditions. For example, psoriasis is a complicated skin disease that strongly concerns the scientific community because of its unclear pathogenesis and the current inability to cure it. The Pharmacogenomics Lab of ETH has been working on the development of psoriatic skin models in order to investigate the driving mechanisms of the disease and to later implement high-throughput drug screening to explore treatment possibilities. However, the manual production into transwell inserts results in unstable, self-contracting and inconsistent skin models, pain points that the Pharmacogenomics Lab would like to eliminate.

The Product Development Group of ETH Zurich, and more specifically the Skin Creator project have developed a skin-producing machine for the automated injection molding of dermal grafts used in clinical applications. A new collaboration between the Product Development Group and the Pharmacogenomics Lab has been recently initiated in an attempt to standardize the fabrication of the psoriatic skin models. For this purpose, this Master Thesis focused on the investigation of the potentials and limitations of the automated injection molding in the generation of consistent and representative dermo-epidermal models for psoriatic skin. Consistency, stability and size maintenance of the hydrogels, viability and distribution of fibroblasts in the dermal matrix, remodeling of the dermal matrix by fibroblasts as well as viability and differentiation of keratinocytes were parameters based on which automated injection molding and manual fabrication were compared.

After a series of experiments, it was seen that in-mold fabrication achieves homogeneous and consistent dermal hydrogels that maintain their dimensions throughout the whole cultivation period regardless of the collagen concentration employed for the dermal matrix, while automated injection molding allows the utilization of collagen concentrations higher than the unstable 5mg/ml, traditionally used in the manual fabrication method. All collagen concentrations exhibited similar biological performance, but the optimum fibroblasts viability was achieved in case of 5mg/mL, meaning that the whole injection molding process should be faster and even simpler to fully prevail over manual fabrication of skin models and better fit the requirements of skin disease research. Keratinocytes viability and differentiation was similar for all mold designs, all collagen concentrations and both fabrication methods. Development of a first psoriatic model, consisting of psoriatic fibroblasts and healthy keratinocytes, did not show any direct effect of diseased fibroblasts on keratinocytes proliferation and differentiation as the epidermal layer of the psoriatic model was very similar to this one of the healthy model.

Evaluation of the automated seeding of keratinocytes for further standardization of the process and elongation of the psoriatic model's cultivation period for a more thorough study should be the next steps. In the long-term, incorporation of all the psoriasis-related cells and molecules in a simple and fast way, as well as further advancements in the mold design to facilitate a direct high-throughput drug screening should be considered.



# Acknowledgments

*Maria Sarkiri  
Delft, October 2018*

I would like to sincerely thank Prof. Mirko Meboldt for giving me the opportunity to participate in this very interesting and challenging project, as well as Stephan Fox for all the useful and on-time guidance he provided as the supervisor of my master thesis.

Additionally, I am grateful to Prof. Michael Detmar for the opportunity to work in his lab for the conduction of the biological experiments, as well as Jihye Kim and Dr. Carlotta Tacconi for the close and flawless collaboration and for all the valuable insight and help they offered me. Besides, I would like to thank the laboratory technician Jeanette Scholl for the training and the aid she gave me in embedding, sectioning and staining processes, while I also owe many thanks to Dr. Sung Sik Lee for the training he provided regarding the plasma sterilization process. And of course, I would also like to thank the whole Skin Creator Team as well as all the members of the Pharmacogenomics Lab for the substantial cooperation and the pleasant moments.

Furthermore, I would like to thank Professors Lidya Fratila-Apachitei and Amir. A. Zadpoor for approving the conduction of my master thesis at the Product Development Group of ETH Zurich, while I sincerely and deeply appreciate all the support and insight that especially Prof. Lidya Fratila-Apachitei offered me throughout the whole exchange period.

Additionally, I feel honestly and deeply thankful to Ms. Gerdien de Graaf and the whole IDEA League team for the provision of the IDEA League Grant which financially supported my stay at ETH Zurich.

Last but not least, I would like to thank my family as well as my closest person, Apostolo Krystallidi, for all the love, support and belief they have been constantly showing to me.



# Contents

<b>Abstract</b>	<b>iii</b>
<b>Acknowledgments</b>	<b>v</b>
<b>1 Introduction</b>	<b>3</b>
1.1 Native Skin . . . . .	3
1.2 Bioengineered Skin. . . . .	4
1.3 Applications of Bioengineered Skin . . . . .	5
1.4 Bioengineered Skin and Psoriasis . . . . .	5
1.5 In vitro Skin Models . . . . .	7
1.6 Fabrication Methods . . . . .	8
1.7 Aim of the Project. . . . .	11
<b>2 Materials and Methods</b>	<b>15</b>
2.1 Cell Isolation . . . . .	15
2.2 Cell Culture . . . . .	15
2.3 Fabrication of Dermo-Epidermal Hydrogels. . . . .	16
2.3.1 Manual Fabrication of Hydrogels . . . . .	16
2.3.2 Automated Injection Molding of Hydrogels . . . . .	16
2.3.3 Forming Molds and Cases . . . . .	17
2.3.4 Air-Liquid Interface Holders . . . . .	18
2.4 Analysing Methods . . . . .	18
2.4.1 Transwell Migration Assay . . . . .	18
2.4.2 Shrinkage Observation. . . . .	19
2.4.3 Fluorescence Microscopy . . . . .	19
2.4.4 Live-Dead Staining . . . . .	19
2.4.5 Histology . . . . .	19
2.4.6 Statistical Analysis . . . . .	21
<b>3 Results</b>	<b>23</b>
3.1 Mold Design Effect on Dermal Hydrogels . . . . .	23
3.1.1 Flaws of Transwell Inserts . . . . .	23
3.1.2 Effect of Shape and Size of Molds on Dermal Hydrogels. . . . .	23
3.1.3 Effects of Membrane Pore Size on Keratinocytes Migration . . . . .	27
3.2 Collagen Concentration Effect . . . . .	28
3.2.1 Shrinkage of Hydrogels . . . . .	28
3.2.2 Fibroblasts Viability. . . . .	28
3.2.3 Fibroblasts Distribution. . . . .	29
3.2.4 Collagen Remodeling . . . . .	29
3.2.5 Keratinocytes Viability and Differentiation . . . . .	29
3.3 Psoriatic Skin Model . . . . .	37
<b>4 Discussion &amp; Outlook</b>	<b>39</b>
4.1 Optimal Mold Design . . . . .	39
4.2 Optimal Collagen Concentration. . . . .	40
4.3 Psoriatic Skin Model . . . . .	42
4.4 Comparison between Automated Injection Molding and Manual Fabrication . . . . .	43
<b>5 Conclusions</b>	<b>45</b>
<b>Bibliography</b>	<b>47</b>



# Abbreviations

ECM	Extracellular Matrix
GAGs	Glycosaminoglycans
3D	Three-Dimensional
2D	Two-Dimensional
RHS	Reconstructed Human Epidermis
DED	De-epidermalized Dermis
IL	Interleukin
HDF	Primary Neonatal Human Dermal Fibroblasts
GFP-HDFn	Green Fluorescence Protein expressing Human Neonatal Dermal Fibroblasts
HaCaTs	Immortalized Human Adult Low Calcium High Temperature Keratinocytes
FACS	Fluorescent-Activated Cell Sorter
DMEM	Dulbecco's Modified Eagle's Medium
FBS	Fetal Bovine Serum
DPBS	Dulbecco's Phosphate Buffered Saline
NaOH	Sodium Hydroxide
NaHCO <sub>3</sub>	Sodium Bicarbonate
NaN <sub>3</sub>	Sodium Azide
DMSO	Dimethyl Sulfoxide
PFA	Paraformaldehyde
UV	Ultraviolet
PET	Polyethylene Terephthalate
ScopeM	Scientific Center for Optical and Electron Microscopy



# Introduction

## 1.1. Native Skin

Skin is the largest organ of human body, covering the whole surface of it. It belongs to the first line of defence, and hence it is an essential part of the immune system. It does not only serve as a barrier preventing the entrance of pathogenic and harmful invaders, but it also hinders the growth of bacteria because of its acidity, while the secretion of antimicrobial peptides, namely defensins, controls the colonization of pathogens when the surface barrier is ruptured <sup>[1]</sup>. Besides, skin performs many other functions; it protects from ultraviolet light absorption, prevents water and electrolytes loss, regulates the body temperature, while it also serves as a sensation organ via the several nerve cells it consists of <sup>[1,2]</sup>.

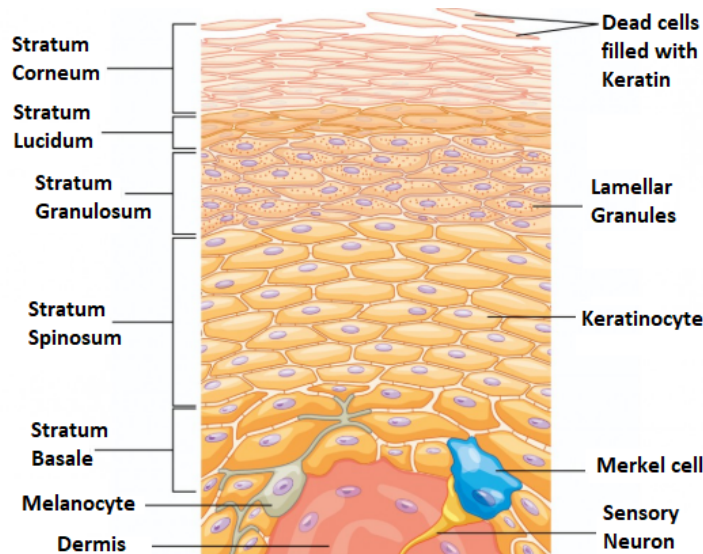


Figure 1.1: The epidermal layer along with the different epidermal sublayers of native skin [3]

Skin is majorly composed of two distinct layers; the dermis and the epidermis. Epidermis is the outer layer of the skin. Its main cell type is keratinocytes, a specific kind of epithelial cells. It also contains melanocytes, Merkel cells and Langerhans cells <sup>[2]</sup>. The different sublayers of the epidermis, from the innermost to the outermost, are the stratum basale, stratum spinosum, stratum granulosum, stratum lucidum and stratum corneum (Figure 1.1). The first sublayer to be produced is the stratum basale, in which differentiation process of keratinocytes begins, and the other sublayers are then formed. The outermost layer, namely stratum corneum, is actually a dead cells-layer, and the basic constituent of the skin barrier <sup>[4]</sup>. Dermis is located under the epidermis. It mostly consists of fibroblasts and the extracellular matrix (ECM) that they secrete. The main component of ECM is collagen type I, while

also elastin and other types of collagen are found [2, 4]. Proteoglycans and glycosaminoglycans (GAGs) are incorporated in the ECM, as well. Although epidermis is avascular and lacks nerves, dermis contains both blood vessels and nerves, as well as, hair follicles, sebaceous and sweat glands, and lymphatic vessels. Dermis serves as support and nutrient supply for the epidermis. The two layers are separated via a basement membrane, namely basal lamina, which controls the exchange of molecules between them [4]. Hypodermis lies under the dermis and it contains fibroblasts, macrophages, and adipose cells, as well as nerves and blood and lymphatic vessels. Its main function is fat storage while it also participates in the adaptive immunity [2,5].

## 1.2. Bioengineered Skin

Bioengineered skin is called an artificially fabricated skin substitute. It is generated by assembling human skin cells into a three-dimensional (3D) matrix. The isolated fibroblasts are embedded in a 3D matrix, and a period of incubation and cultivation allows their attachment, development, and reorganization in the matrix so that a dermal equivalent arises. Keratinocytes can be then seeded on top of the dermal equivalents to generate a full dermo-epidermal substitute. Following cultivation at air-liquid interface results in keratinocytes differentiation and formation of several epidermal sublayers. Collagen type I usually composes the artificial matrix due to its abundance in dermal ECM, while fibrin is also regarded as a good option thanks to its primary synthesis during blood clotting and healing process [6-8]. Also, synthetic polymers are sometimes selected as the scaffolds carrying skin cells, thanks to their good mechanical properties and stability [8].

The history of bioengineered skin is already long. Several skin substitutes are nowadays commercialized, while plenty laboratories in universities and medical centres continue the research to improve their quality and properties [5]. However, most of them include currently only the epidermis and/or the dermis, composed of allogenic cells. Epidermal equivalents are quite fragile, and keratinocytes proliferate slower in the absence of fibroblasts, while dermal substitutes lack the outer protective skin barrier. Full-thickness dermo-epidermal equivalents are more representative and have been proved to improve and accelerate the healing quality in clinical use [8].

However, even full-thickness dermo-epidermal equivalents are still a simplified representation of human skin. Figure 1.2 depicts anatomical differences between native and a paradigm of bioengineered skin. Significant effort is currently given to the incorporation of other cell types found in skin tissue to promote also vascularization, pigmentation, innervation and lymphangiogenesis in the skin model so that it further mimics human skin structure and function. A big challenge remains the inclusion of skin appendages, like hair follicles, sweat and sebaceous glands [9].

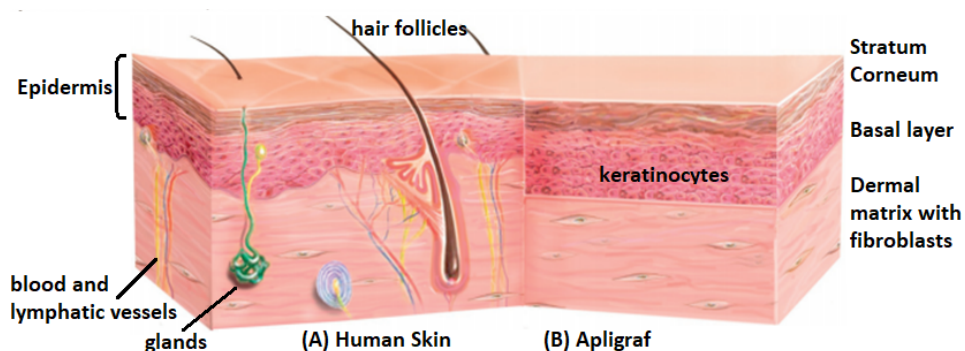


Figure 1.2: Anatomic differences between native skin (left) and an example of dermo-epidermal equivalents, namely Apligraf (right) [10]. A typical dermo-epidermal equivalent includes a dermal matrix with embedded fibroblasts and the different sublayers of the epidermis, but it lacks the hair follicles, sebaceous and sweat glands, blood and lymphatic vessels, as well as the nerves of native human skin.

### 1.3. Applications of Bioengineered Skin

The initial and basic reason for development of bioengineered skin has been the acute or chronic wounds mostly caused by burn injuries [11, 12]. The gold standard regarding the treatment of these wounds has been the autografting. Autografting includes transplantation of a healthy autologous skin piece, removed from an undamaged body area of the patient [5]. Therefore, it is a painful and slow method of treatment that demands several surgeries, resulting in patient pain and discomfort. Additionally, in case of large wounds, autograft size does not suffice to cover all the injured area [5, 12, 13]. Allografts is not fully efficient alternative due to the donor shortage and the risk of rejection, while xenografts set risks related to the species differences [13]. These facts have resulted in the generation of bioengineered skin substitutes that could overcome the above difficulties. They are designed to close the wound temporarily or even permanently, restoring the skin barrier and preventing pathogens invasion [4, 13]. In order for it to be efficient and superior alternative to standard treatment methods, bioengineered skin must be stable, abundant, reproducible and available in different sizes, while it should serve as a good analogue of native skin [4]. Skin grafts vary from simple epidermal transplants or acellular scaffolds occupied by the patients' cells after transplantation, to full dermo-epidermal equivalents [8]. The more similar to the native skin, the better the quality and cosmetics of the graft and the faster the initiation of the healing process. And though the perfect skin substitute has not been developed yet, several successful transplantations of bioengineered skin have been achieved, not only in patients with burn injuries but also in people suffering from dermatological disorders, like diabetic ulcers [14].

Although bioengineered skin was firstly developed for clinical application in reconstructive surgery [11, 12], it is now also considered as a potential skin model in research. For example, it is used for preclinical testing of drugs and cosmetic products to predict their *in vivo* performance and hence, ensure efficacy and safety [4], while it is considered as a suitable platform for conducting high-throughput screening [15].

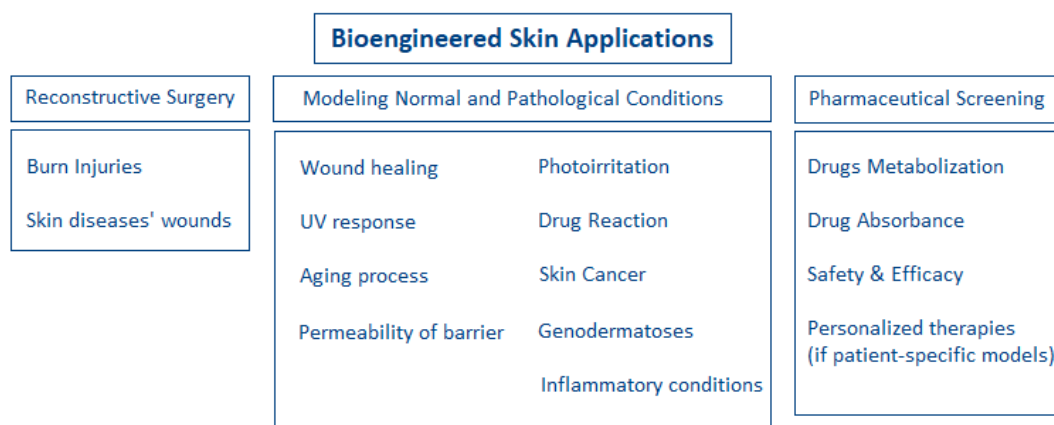


Figure 1.3: Diagram of the different applications of bioengineered skin in the areas of reconstructive surgery, modeling of physiological and pathological skin conditions, and pharmaceutical screening.

Besides, skin models can be beneficial for the modeling of several physiological and pathological skin conditions [4, 11, 16]. For example, the wound healing process could be reproduced *in vitro* in the context of regenerative medicine to assess and predict *in vivo* events, while response to ultraviolet irradiation could be assessed to determine its riskiness. Finally, skin substitutes are now regarded as a useful platform for the modeling of complicated and severe skin diseases and for the pre-clinical assessment of potential therapies [4, 16, 17]. Figure 1.3 summarizes the different applications of bioengineered skin nowadays.

### 1.4. Bioengineered Skin and Psoriasis

One of the severe dermatological disorders that strongly concerns the scientific community because of its unclear pathogenesis and incurable character is Psoriasis [18-20]. It affects

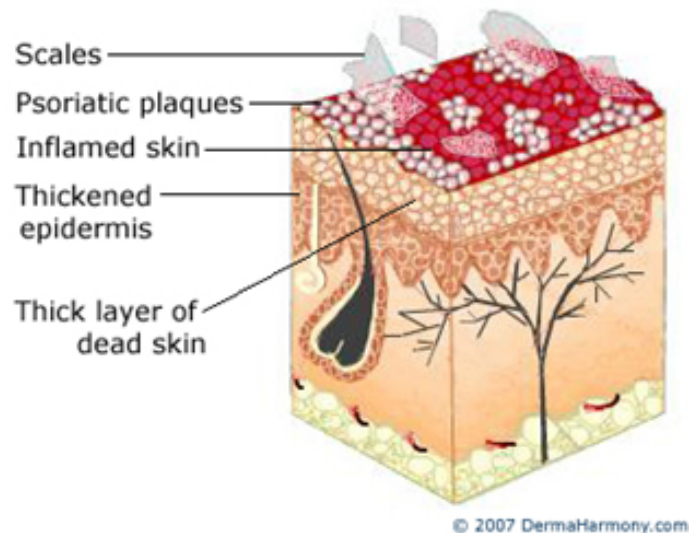


Figure 1.4: Structure of skin affected by plaque psoriasis, including a thicker epidermis, reddish colour of skin, whitish scales on top, inflamed dermis and epidermis [25].

about 2% of the world population [19]. The disease has different types but plaque psoriasis accounts for most of the cases. Figure 1.4 depicts the morphological changes of skin in plaque psoriasis. In this type, the lesions are thick enough, red-coloured in their base with white scales on top, circularly-shaped, and mostly found in knees, elbows and the scalp in several sizes. Pathogenesis of the disease is still unclear, but it is supposed to result from an interplay between the immune system, the skin cells, as well as, genetic and environmental triggers. In case of infections, like streptococci, or physical trauma, like burn injuries, there are more possibilities for the disease occurring, while conditions, like stress, may also play a role [19].

Psoriatic symptoms vary in the different types of the disease, with irregular patches and itching being generally common. The disease has negative impact on patients' psychology, and hence it may adversely affect their social life or even lead to depression. Moreover, it is strongly associated with co-morbidities, like obesity and the metabolic syndrome. In some cases, side-effects or even deterioration of the disease may occur from the same the treatment [20]. Despite the several available systemic and local treatments, no permanent cure has been developed so far, and only limitation of symptoms has been achieved [19]. The first to be done is to understand the driving mechanisms of the disease. As the pathogenesis of psoriasis seems to be complicated, there are various parameters that could be investigated. For example, there are indications that diseased fibroblasts affect keratinocytes differentiation and proliferation, leading to the generation of the abnormal psoriatic lesions [21, 22], while there are several cytokines released by immune and skin cells that are supposed to play driving role [23, 24].

For the thorough investigation of the interplay between the large number of probably involved cytokines, the skin cells and the immune system, skin models are required. Human skin would be the ideal model, but *in vivo* studies are restricted for safety and ethical reasons. Also, the use of animal models is limited not only due to ethical considerations, but also due to the poor resemblance of human skin, and therefore the debatable reliability of studies' outcomes [26]. Cadavers or biopsies of patients are sometimes used for preclinical studies, but the available specimens might not suffice in size or quantity for an extensive research, whereas the heterogeneity between specimens coming from different individuals is a downside when repeatability is required [26]. The *in vitro* reconstruction of a consistent and representative skin model could help overcome these limitations. Utilization of human cells and of an extracellular matrix providing the necessary 3D environment for the normal growth, proliferation, and function of the cells achieves a more representative model than

2D cultures or animal models, without posing ethical doubts [16, 26]. Besides, a single biopsy can result in a wealth of cells after their in vitro expansion and cultivation, allowing the fabrication of adequate number of skin models, having the same origin, and thus availability and repeatability issues are solved. What else is important is the generation of consistent skin models facilitating the reliable research of psoriasis and other dermatological disorders [2, 18], and this requirement is highly related to the fabrication process. Finally, due to the high complexity of psoriasis, a thorough research would benefit from the incorporation of several molecular and cellular skin components in the skin model, which remains still a challenge in the development of bioengineered skin.

## 1.5. In vitro Skin Models

As already discussed, current applications of bioengineered skin are not restricted to reconstructive surgery but are expanding in the areas of pharmaceutical screening and modeling of normal and pathological skin conditions. Several types of bioengineered skin can be employed based on the pathogenesis of the disease studied and the research goals. When applicable to the investigation of dermatological disorders and their potential medications, they are called in vitro skin models. Their main drawback lies in their structural simplicity, especially in case of complex skin diseases, like psoriasis or skin cancers, the pathogenesis of which results from complicated interactions between cellular or molecular components [28]. Reliable and beneficial modeling of skin diseases demands a robust, standardized and representative 3D model [29]. A brief overview of available bioengineered skin types applicable to skin disease modeling is presented below.

- Monolayer models are consisting of a single cellular type; either fibroblasts or keratinocytes, representing the dermis or the epidermis, respectively. They offer the capability to study the physiology or pathogenesis of each cell type separately, whereas they partially allow the investigation of cellular interactions by revealing cell behaviour in the absence of other cell types. For example, when Chiricozzi et al. studied the effect of IL-17, a psoriasis-related cytokine in keratinocytes monolayers and in full thickness equivalents, they detected a stronger psoriatic effect on the full thickness model [30]. Monolayers lack the 3D environment that is important to the normal growth and function of cells, while they cannot model the interplay between dermis and epidermis [31, 32].
- Reconstructed human epidermis (RHS) is a skin model consisting of a membrane, made of polycarbonate, in which keratinocytes are seeded and then cultured at air-liquid interface in order for differentiation to take place and for the epidermal sublayers to be formed. It is a 3D equivalent but like monolayers, it cannot study the interactions between keratinocytes and other skin cells [33].
- De-epidermalized dermis (DED) occurs when after biopsy the epidermis is separated from the dermis. Keratinocytes can be later seeded on top of DED, which is usually acellular, and after cultivation at the air-liquid interface, a differentiated epidermis is formed, resulting in a 3D full dermo-epidermal equivalent [34, 35], which is a closer representation to native skin.
- Collagen hydrogels is a well-known type of skin substitutes, having also clinical applications [4]. Human fibroblasts are embedded in a collagen hydrogel, offering the necessary 3D environment, and after a period of incubation and cultivation, they re-organize the dermal matrix and a simple reconstructed dermis occurs. On top of it, keratinocytes are seeded to acquire a full dermo-epidermal equivalent that better applies to the research of skin diseases. Incorporation of more cells found in skin tissue into the reconstructed dermal matrix is required for the modeling of most skin disorders.
- Self-assembled models occur when human fibroblasts are let in culture to produce their own extracellular matrix (ECM), and then keratinocytes of the same source are seeded on the dermis. This method has managed to successfully generate for example psoriatic skin models when diseased skin cells were utilized [31, 32]. They are the best representation of native skin thanks to the fully autologous source of cells and biomaterials, but

their efficacy depends on fibroblasts capability to produce sufficient amount of ECM, which takes considerable time <sup>[31]</sup>.

- Skin-on-chip models are more complex structures, useful for the in vitro modeling of complex skin diseases. They may differ in structure based on the incorporated and studied cellular and molecular components but usually the different cell types are cultured in different layers or chambers of the same platform, which communicate and interact with each other through porous membranes. They also contain microfluidic devices, like micro-valves and mixers, that control nutrition of the cells as well as interchange of molecules between the different layers of the model, trying to mimic the operation of skin tissue <sup>[36-38]</sup>.

## 1.6. Fabrication Methods

Production of bioengineered skin, either in case of skin grafts or in case of skin models, has been traditionally conducted manually; from the isolation of cells to the assembly of them in 3D matrix and the in vitro generation of the skin analogues. There are different fabrication approaches that are followed. As already mentioned, in most cases collagen hydrogels are generated, as they resemble the stiffness of skin tissue and resist high amount of water <sup>[39]</sup>. Plastic compression is a method developed by Brown et al. <sup>[40]</sup> and optimized later by Brazilius et al. <sup>[13]</sup> for the prevention of high contraction and instability that are usually detected in hydrogels. In this method, the initially thick dermal hydrogels are compressed to reach a final thickness of maximum 1mm prior to the keratinocytes seeding. The compressive platform can vary in size, thus allowing the fabrication of skin substitutes in several sizes based on the specific need <sup>[13, 40]</sup>. Compression of the hydrogels is carried out manually, and hence it can be laborious. In the self-assembly method, fibroblasts are let to secrete their own ECM and a fully autologous dermal equivalent occurs as no biomaterial is added. In most cases, the generated ECM sheets that fibroblasts produce in culture are very thin, and the final dermal matrix results from manual superposition of several sheets together, a quite tedious process. The amount of time demanded for the formation of this skin model is high; several weeks may be needed for sufficient quantity of ECM to be generated <sup>[31, 32]</sup>.

Regardless of the exact approach, the manual character of the processes is a downside. Manual fabrication is not only considered as time-consuming and laborious for the researchers, but it also shorts on accuracy and consistency <sup>[2]</sup>. Pipetting variabilities between different individuals or between different time points have been recorded in relevant experiments <sup>[41]</sup>. In general, two different individuals cannot be proved to perform precisely the same procedure, while even the same person cannot fully standardize his motion. In case of high-throughput pharmaceutical screening and skin disease modeling, a wealth of same skin models is required for adequate and reliable experiments to be conducted, and manual fabrication does not ensure the satisfaction of this demand <sup>[42]</sup>. Need for time savings, decrease in manual labor and mainly, standardization of the process in order for repeatable and consistent skin models to be produced has resulted in efforts to automate the fabrication of bioengineered skin <sup>[2, 43]</sup>. Also, rapid research and large scale studies would profit from an automated and non-complex fabrication process that could be easily adjusted and modified based on the research needs, while also allowing easy troubleshooting and maintenance.

- Robotic Production: In some laboratories, replacement of humans by robots is currently attempted <sup>[15, 46]</sup>. Figure 1.5 illustrates a relative paradigm, in which a dual-arm robotic system executes pipetting and other biological tasks <sup>[44]</sup>. The Fraunhofer team has generated the Skin Factory, in which all fabrication steps, ranging from sterilization of the skin biopsies to the assembly of the cells in the 3D matrix, are carried out by a robotic arm with no participation of humans <sup>[15, 42]</sup>. The same group has managed to automatically generate human epidermis models with the use of robot <sup>[14]</sup>. This approach has resulted in significant decrease of manual work and standardization of the production process, given that a programmed robot can constantly perform all steps with fixed speed and fully-controlled motions <sup>[15, 44]</sup>. Despite the automatic character of the process, it still remains time-consuming, given that it includes the same steps with

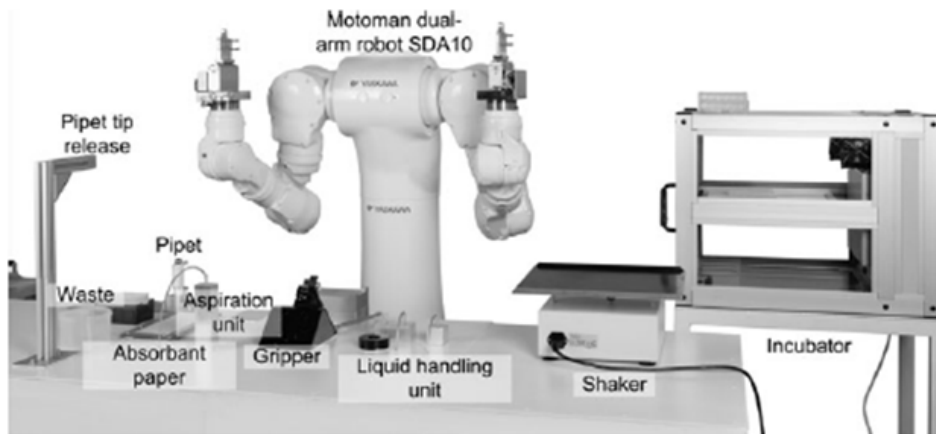


Figure 1.5: Execution of manual laboratory work by robot [44].

manual fabrication, but human hands are replaced by robotic arms. Another drawback of this method is that robots are barren of human adaptability. The complexity of robotic operation demands constant recruitment of specialized staff for repair, maintenance or re-programming of the robots for any change in the fabrication protocol, resulting in unavoidable time delays.

- 3D bioprinting of skin is currently an emerging research area regarding the automated fabrication of skin models [2, 27, 43]. There are various 3D bioprinting methods, each of which overrides or shorts on in different aspects. All of them can be categorized according to the main biofabrication approaches: the bottom-up and the top-down approach. In the bottom-up approach small cellular and non-cellular building blocks are arranged in space in a way that a larger 3D biomimetic model is formed. The top-down approach includes seeding of cells along with deposition of suitable biomolecules on larger biodegradable construct so that the cells can eventually form their own 3D matrix that will replace the initial construct. The latter approach can result in a strongly biomimetic model, but it demands significant time-investment [2]. There are three major bioprinting categories which are applied to the fabrication of bioengineered skin; laser-assisted bioprinting, inkjet bioprinting, and extrusion bioprinting. Figure 1.6 is simplified visualization of their operation concept.

**a. Laser-assisted bioprinting** exploits laser energy to print. Small droplets of cells are printed in a substrate that can be either a cell culture plate for generation of 2D construct or a scaffold for formation of 3D construct. Precise deposition of the cells in the 3D construct in a high density is achieved while there are no limitations in the biomaterials viscosity. Several dermo-epidermal skin substitutes have been already successfully fabricated by this method [2, 27]. A downside of laser-based bioprinting is the relatively low printing speed [2].

**b. Inkjet bioprinting** is based on the ejection of bio-ink droplets in a substrate. Bio-ink contains cell suspension combined with hydrogels or biopolymers. In thermal inkjet bioprinting the droplets are pushed out due to bubbles generated in the nozzle by a heating element, while in piezoelectric inkjet bioprinting, electric pulses result in the droplets ejection [2]. Thermal inkjet printing is considered suitable for biological applications as the printed cells are heated in a temperature less than 10° above ambient temperature and for only 2 microseconds, ensuring cell survival during the printing and a later cell viability of about 90%, while piezoelectric approach operated in frequencies that can harm the cells [38]. Inkjet bioprinting can achieve high resolutions and accuracy in deposition but it is efficient only when bio-inks of low viscosity are printed [2].

**c. Extrusion bioprinting** is based on the extrusion of a continuous strand of biopoly-

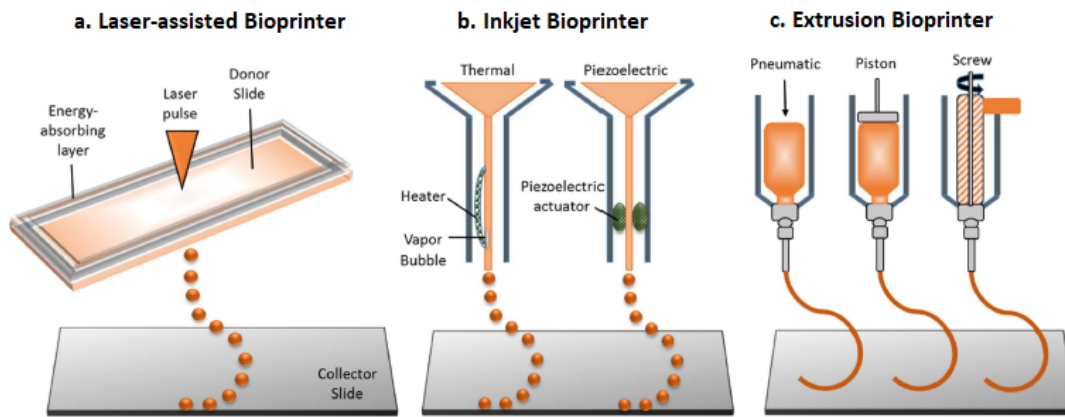


Figure 1.6: Illustration of three major categories of 3D bioprinting. (a) Laser-assisted bioprinting, in which laser pulses on the donor slide result in material deposition in the collector slide. (b) Inkjet bioprinting, in which either heating or electric pulses lead to the injection of bio-ink on the substrate. (c) Extrusion bioprinting, in which a mechanical force (pneumatic, screw-driven or piston-driven) causes the extrusion of biomaterials on the substrate [2].

mers or hydrogels, along with cellular components when desired, through a nozzle when mechanical force is applied. Simultaneous printing of cells, biomaterials and growth factors can be achieved in systems of more than one extruder, contributing to the generation of a more complex skin model. This approach is considered faster than inkjet and laser-based bioprinting, while it is suitable for generation of anatomically relevant structures and sizes [2, 45]. It also works with high cell density though shear stresses developed in the nozzle may reduce cell viability. Comparison between 3D extrusion bioprinting and manual deposition of skin components has concluded to the better long-term maintenance of skin equivalents shape and size in case of the 3D printing approach [2]. However, this method shorts on resolution capabilities compared to other bioprinting techniques, which affect the precision in cells' spatial arrangement [46].

Regardless of the specific method, 3D bioprinting offers the capability of massive production of robust and consistent 3D skin models in an automated way, that is faster from manual or robot-assisted fabrication methods [2, 27, 43, 47]. Besides it facilitates the incorporation of several molecules and cell types promoting also pigmentation, innervation and vascularization, which are important aspects of strongly biomimetic skin equivalents [48]. Scalability is another advantage of 3D-printing approach that benefits high-throughput pharmaceutical screening, while patient-specific skin substitutes can be still fabricated by printing autologous cells, contributing to research of personalized therapies [2, 27]. Despite all the advantages, 3D printers are high-complexity systems, demanding the recruitment of specialized personnel for sterilization, maintenance or troubleshooting, while costs for constant supply of tools and biomaterials which are in proper fluidity and viscosity to be printed are considerable [2].

- Automated Injection molding is another approach, recently developed by the Product Development Group, Zurich [49, 50]. It has been based on the plastic compression method of Brazilius et al. [13] but it employs a different technique for avoiding the high contraction of the formed collagen hydrogels. Fibroblasts and high-concentration collagen, instead of unstable low-concentration collagen [13], are mixed and injected into closed molds of 1mm thickness, while in-mold cultivation and incubation follows to avoid contraction and maintain size and shape of the dermal hydrogels [50, 51]. A skin-producing machine is used for the automatic mixing and injection of the dermal components into the molds, which is considerably faster than manual plastic compression process [49, 51]. Consistent dermal equivalents are achieved while scalability could be accomplished with variations in molds' shape and size. Figure 1.7 portrays



Figure 1.7: Components of injection molding process. Left: Double cartridge, containing high concentration collagen in the left container and fibroblasts suspension in the right container, along with a mixing nozzle in which the contents are mixed and then injected into the encased mold. Middle: in-mold dermal hydrogel (pink colour due to fibroblasts culture medium). Right: Device for automated fabrication of dermal equivalents.

the skin-producing machine, the cartridge filled with the skin constituents and an in-mold dermal hydrogel. The next-generation device, in which keratinocytes seeding is also automated, is currently being developed and assessed [52]. Keratinocytes' seeding, either manual or automated, is carried out without removing the molds so that in-mold cultivation of dermo-epidermal models follows, aiming to minimization of manual steps until final use. The device has been developed such that it offers a friendly user interface and can be easily used by the same the researchers, while a wide range of settings in terms of flow speed and volume of injected components allows the immediate adaptation to simple changes in the fabrication protocol without re-programming. However, the time savings of this method are limited to mixing and injection of skin constituents, while the rest steps are still conducted manually [51]. This skin-producing machine is just one part of a bigger project, called Skin Creator, which plans to automate the whole process of bioengineered skin fabrication, from skin biopsy to maturation of skin analogues prior to transplantation, so it promises a fully-automated solution in the future.

## 1.7. Aim of the Project

Slow production pace and doubtful consistency of skin models in case of traditional manual fabrication has led to development of automatic production methods, ranging from robotic systems to 3D printing techniques. Standardization of the fabrication process, scalability and personalization capabilities are essential to applications like skin disease modeling and high-throughput pharmaceutical screening. Besides, low complexity of the production system may facilitate use and fast adaptation to the research needs, supporting rapid progress and hence the fabrication methods as well as the produced skin models should be capable of satisfying these requirements.

Regarding specifically psoriasis, its modeling takes place in 2D cultures of human epidermal keratinocytes, epidermal monolayers or dermo-epidermal models in the form of hydrogels or self-assembled models [53-55], which are still fabricated manually. The keratinocytes-based models are mostly used to detect keratinocytes response to specific cytokines and inflammatory triggers but as already mentioned they lack the physiological 3D environment and cellular interactions of native skin. Besides, the dermo-epidermal hydrogels usually suffer from instability and self-contraction [13], while the self-assembled models demand a lot of time to be produced especially in large quantities that large scale studies require. Additionally, the manual production of all these models is generally laborious and not standardized, doubting the outcomes of the research.

The Pharmacogenomics lab of ETH, Zurich has been lately involved in generation of psoriatic skin models in the form of hydrogels aiming to investigate the driving mechanisms of

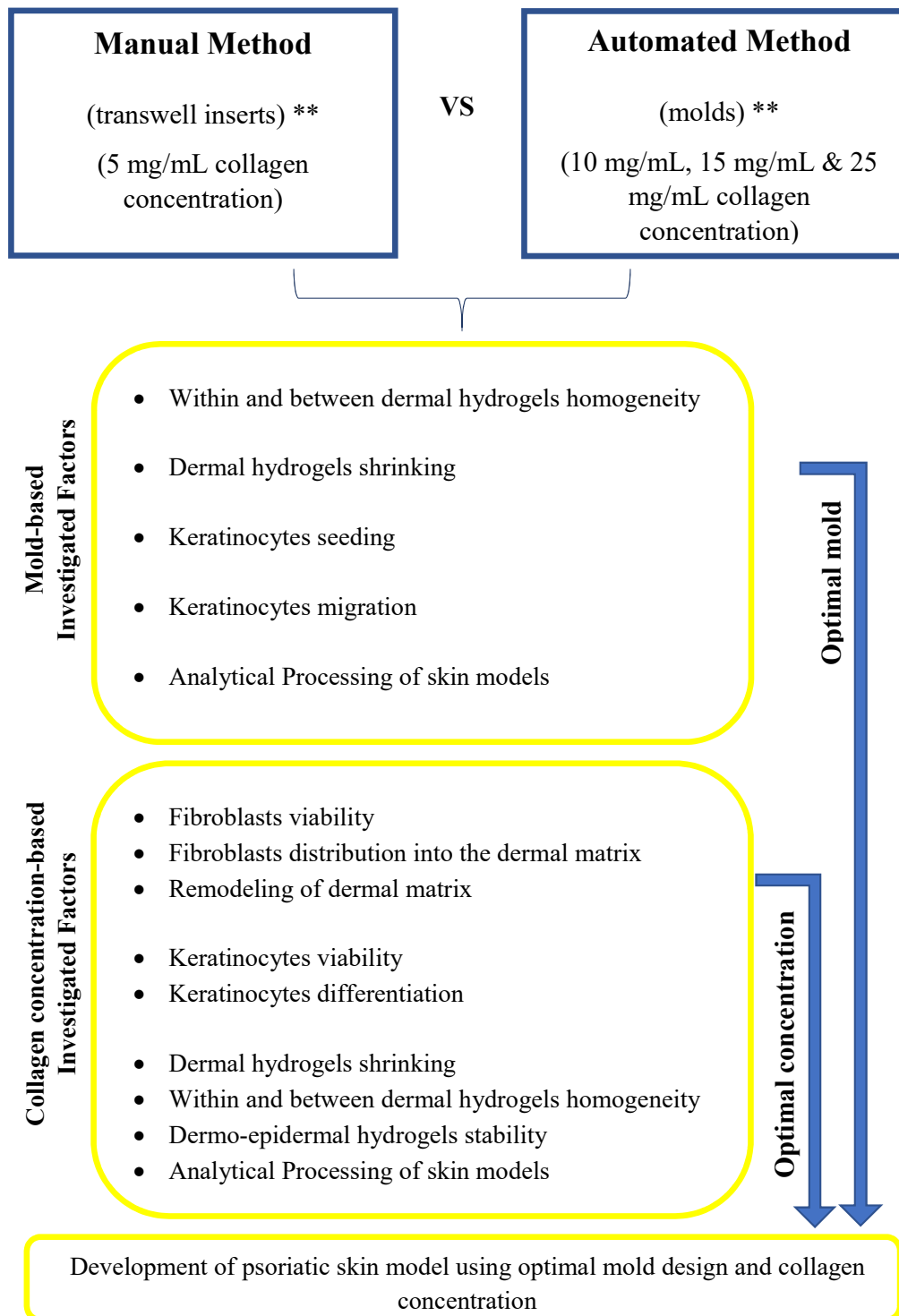
the disease and proceed later to high-throughput drug screening for development of potential medications. The goals of their research include firstly the examination of the direct effect of psoriatic fibroblasts on healthy keratinocytes as well as the role of cytokines IL-17 and TNF-alpha, that have been widely discussed on literature, in the initiation and progression of the disease [56, 57]. Vascular endothelial cells and lymphocytes are planned to be also incorporated in the dermo-epidermal models to properly represent the disease. The main problems they have faced during the manual fabrication of their models is the high-self contraction of the hydrogels and the inconsistency between different samples. A recent collaboration between the Pharmacogenomics Lab and the Product Development Group of ETH Zurich has generated opportunities for automated injection molding of skin models applicable to psoriasis research in an effort to solve the instability and inconsistency issues that come from the manual fabrication of hydrogels in a non-complex and non-expensive way. The method of automated injection molding was initially inspired and developed by the Product Development Group for the fabrication of dermo-epidermal grafts applicable to reconstructive surgery. Automated injection molding results in very stable and consistent dermal grafts in which keratinocytes are later manually seeded for a full dermo-epidermal graft to occur, while shortly this seeding will be also made automatically.

The general aim of this research was to compare the automated injection molding and the manual fabrication method regarding the development of dermo-epidermal models applicable to psoriasis research. Briefly, manual fabrication included pipetting and stirring of fibroblasts suspension, collagen solution in a concentration of 5mg/mL and a reconstitution buffer enabling the gelation of the samples. After stirring, the skin mixture was pipetted into transwell inserts, and after some days manual seeding of keratinocytes on top of the formed hydrogels followed. Exposure to the air-liquid interface a few days after the keratinocytes seeding mediated the differentiation of the keratinocytes. Automated injection molding on the other hand involved a device which automatically mixes and injects into molds a collagen solution (in a concentration of 10mg/mL, 15mg/mL or 25mg/mL), a chemical hardener for the gelation and the fibroblasts suspension. Some days later manual seeding of keratinocytes on the bottom of the in-mold hydrogels followed and exposure to the air-liquid interface a few days after the keratinocytes seeding mediated the differentiation of the keratinocytes. Automated injection of dermal components into transwell inserts as well as manual pipetting of dermal components into molds were also tried to specifically evaluate the benefits of the molds.

The specific objectives of this research were:

- To assess the effects of mold design on (i) dermal hydrogels shrinking, (ii) within and between hydrogels homogeneity, (iii) efficiency of automated injection of skin constituents, (iv) keratinocytes seeding, (v) migration of keratinocytes through the pores of the mold membrane, and (vi) ease of manipulation of the hydrogels during analysis.
- To investigate the effects of collagen concentration on (i) fibroblasts response, (ii) collagen matrix remodelling by fibroblasts, (iii) keratinocytes viability and differentiation, (iv) dermal hydrogels shrinking, (v) within and between hydrogels homogeneity and (vi) hydrogels stability and ease of manipulation during analysis.
- To develop a psoriatic skin model by combining psoriatic fibroblasts with healthy keratinocytes.

Figure 1.8 summarizes the objectives of the project. The overall goal was the detection of the advantages and mainly limitations of the current automated injection molding method so that the process can be improved in the future in order to serve the overall purpose of the two groups collaboration; the faithful and insightful psoriasis modeling.



*\*\*Automated Injection into transwell inserts as well as manual pipetting into molds were also tried.*

Figure 1.8: Schematic diagram of research approach followed for the investigation of the automated injection molding regarding the development of dermo-epidermal models for psoriasis research.



# 2

## Materials and Methods

### 2.1. Cell Isolation

For the generation of the skin equivalents studied in this Master Thesis, the following cells have been recruited: Primary human dermal Fibroblasts (HDFn) isolated from human healthy skin samples, Green Fluorescence Protein expressing human neonatal dermal fibroblasts (GFP-HDFn) (Cat. No: cAP-0008GFP, ANGIO-PROTEOMIE), Patients-derived Healthy Dermal Fibroblasts, Patients-derived Psoriatic Dermal Fibroblasts, Immortalized human adult low calcium high temperature keratinocytes (HaCaTs).

Primary human healthy and psoriatic fibroblasts were isolated from human healthy skin samples and psoriatic skin lesions of patients suffering from psoriasis vulgaris separately using Dynabeads recognizing CD31 to separate endothelial cells from other skin cells including fibroblasts. Purity of these cells were confirmed by measuring the positivity for PDGFR $\alpha$ , a marker for fibroblasts, by Fluorescent-Activated Cell Sorter (FACS). Contamination by other cell types was excluded based on FACS stainings for intergrin alpha 6 (CD49f), a marker for keratinocytes, and CD31, a marker for endothelial cells. Approval by the UZH Ethics Committee and informed consent by the patients were obtained.

The cells were cultured in Dulbecco's Modified Eagle's Medium containing 4.5g/L D-Glucose, L-Glutamine and Pyruvate (DMEM; Gibco, Life Technologies, Carlsbad, USA) supplemented with 10% fetal bovine serum (FBS; Gibco) and 1% antibiotic antimycotic solution (Gibco).

### 2.2. Cell Culture

Cryopreserved Fibroblasts and HaCaT cells were thawed by immersion of cryovials carrying the cells into 37 °C water bath for approximately 1 minute and addition of sufficient amount of pre-warmed at 37 °C growth medium. The cells were centrifuged at 4 °C and 1000 rpm for 5 minutes, the supernatant was aspirated, and the cells were resuspended in growth medium. The cells were grown at 37 °C and 5% CO<sub>2</sub> incubator, and the growth medium was refreshed every two days.

Prior to the generation of skin equivalents, detachment of the cells from the flasks was performed when the cells in culture reached 80-90% confluency. The growth medium was aspirated and Dulbecco's Phosphate Buffered Saline (DPBS; 1x free of CaCl<sub>2</sub> and MgCl<sub>2</sub>, Gibco) was added to wash the flask and then it was aspirated. 0.05% Trypsin-EDTA (Gibco) was added and the cells were incubated for 5 minutes at 37°C and 5% CO<sub>2</sub>. When the cells were detached, the growth medium was added and thoroughly mixed with the Trypsin to de-activate it. The detached cells were transferred into a falcon tube and centrifuged for 5 minutes at 1000 rpm at 4 °C. After centrifugation, the supernatant was aspirated, and the cells were resuspended in growth medium in concentration dependent on the needs of the experiment.

The fibroblasts were used for up to passage eight.

## 2.3. Fabrication of Dermo-Epidermal Hydrogels

### 2.3.1. Manual Fabrication of Hydrogels

Dermal hydrogels were manually fabricated by thorough mixing of 5 mg/mL concentrated bovine collagen solution (Type I Acido Soluble Collagen, ACI100/5mg, Symatase), reconstitution buffer (0.22gr.  $\text{NaHCO}_3$  and 0.477gr. HEPES in 0.05N NaOH), and cell suspension in 10X-concentrated P-media (DMEM (10x, Sigma)/ Ham's F12 Nutrient Mixture (Powder, ThermoFisher) (3:1)) in a volume ratio 8:1:1, respectively. After thorough stirring of the mixture to reach homogeneity, the volume of 200  $\mu\text{L}$  was pipetted into one 12 mm transwell with 0.4  $\mu\text{m}$  pore polyester membrane insert, while the volume of 1mL was pipetted into a circular mold of 23 mm diameter and the volume of 400 $\mu\text{L}$  was pipetted into each insert of a 23mm x 6mm rectangular mold. Pipetted fibroblast density was 500cells/ $\mu\text{L}$ . An incubation period of 30 minutes at 37 °C followed in order for curing to take place. After this incubation period, fibroblast growth medium was added, and the gels were transferred into a humidified incubator (37 °C, 5%  $\text{CO}_2$ ). Growth medium was replaced every two days.

After 4 days of incubation (37 °C, 5%  $\text{CO}_2$ ), 300'000 HaCaTs were manually seeded on top of gels formed into one transwell of 12 mm diameter or in the bottom of gels formed into rectangular molds, while 900'000 HaCaTs were seeded in the bottom of gels formed into one circularly-shaped mold of 23 mm diameter. Seeding of keratinocytes was made by manual pipetting. Cultivation of the gels submerged (immature state) into fibroblast growth medium followed in a humidified incubator (37 °C, 5%  $\text{CO}_2$  ) for 3 days, and then the gels were transferred at the state of air-liquid interface (mature state) for 5 more days of incubation. At the air-liquid interface, keratinocytes differentiation medium (DMEM (1x, Sigma)/Ham's F12 media (Gibco) (3:1), containing 5% FBS, 4 $\mu\text{g}/\text{mL}$  hydrocortisone (50 $\mu\text{L}$ , Sigma),  $10^{-10}\text{M}$  cholera toxin (50 $\mu\text{L}$ , Sigma) and 20mL 100x Cocktail (5 $\mu\text{g}/\text{mL}$  transferrin (50 $\mu\text{L}$ , Sigma), 5 $\mu\text{g}/\text{mL}$  insulin (50 $\mu\text{L}$ , Sigma),  $2 \times 10^{-8}\text{M}$  Triiodothyronine(2mL, Sigma) and 14mL DPBS) was added in such a quantity that only the free of keratinocytes surface of the gel was in contact with it, while the other surface was free of medium. Keratinocytes differentiation medium was replaced every two days.

### 2.3.2. Automated Injection Molding of Hydrogels

Dermal hydrogels were also fabricated by automated mixing and injection molding of bovine collagen solution, CV buffer (2.2gr.  $\text{NaHCO}_3$  , 4.78gr. HEPES, 0.6gr. NaOH in 100mL ddH<sub>2</sub>O) and cell suspension in fibroblast growth medium. The collagen solutions of different concentration were fabricated by manually dissolving 25mg, 15mg or 10mg of collagen fibers (FIBUS500 Collagen type I, Symatase) into 1mL of 0.0613M acetic acid solution. The collagen solution was loaded in the big chamber of the double cartridge, while the small chamber carried CV buffer and cell suspension mixed in a ratio 2:1 by manual pipetting. For a total volume of 3mL in the small container, 5mL of collagen solution were loaded in the big chamber. After stirring and dissolving the fibers, centrifugation at 3300 rpm and 4°C for 150 minutes followed for removal of bubbles and homogenisation of the solution. The 25mg/mL, 15mg/mL or 10mg/mL concentrated collagen solutions were stored at 4°C until injection, while CV buffer and cell suspension were mixed and loaded in the cartridge right before the injection. The pistons were inserted, and the chambers were vented by holding the cartridge upside-down during the insertion. Then the cartridge was combined with the mixing nozzle and was placed in the appropriate reception of the device so that the injection molding could begin. For the filling of the 23mm diameter circular mold, a total volume of 1000 $\mu\text{L}$  was set in the device settings, while for the filling of a 23mm x 6mm rectangular mold, 400 $\mu\text{L}$  were selected. The desired volume was defined in the device settings by selecting "Bolus Size" and using the up and down arrows to increase or decrease the displayed volume. The flow rate was also adjusted by selecting "Set Flow Rate" and using the up and down arrows to increase or decrease it. A flow rate of 5000 $\mu\text{L}/\text{sec}$  was selected to push the plunger until it touched the pistons, while a flow rate of 250 $\mu\text{L}/\text{sec}$  was chosen for the injection of the skin constituents into the mold. The constituents were mixed and injected by pressing the right arrow of the device, indicated with the name "Infusion". The first 1 mL that was injected was discarded to ensure that both pistons were in the same height and the skin constituents were injected

into the mold in proper volume ratio (2:1).

During injection, the encased molds were positioned on a base so that no manual holding is needed. The base was fabricated by wooden plates which are laser-cut and glued together, while having a flexible polystyrene top surface of 1mm fixed in space with plastic tie wraps. Prior to injection, the outer surfaces of the device and the base were sprayed with 70% Ethanol and then exposed under UV light for 60 minutes, while all the individual components, like pistons, mixing nozzles and cartridges were autoclaved before use. After 5 minutes at room temperature, the cases were removed, and every in-mold gel was placed into a 60mm petri-dish and 6mL of fibroblast growth medium were added. Curing of gels happened immediately after combination of CV buffer and collagen solution and no incubation time was demanded for gelation. Cultivation of the gels in a humidified incubator (37 °C, 5% CO<sub>2</sub>) followed. Growth medium was replaced every two days.

After 4 days of incubation (37 °C, 5% CO<sub>2</sub>), 900'000 HaCaT cells were seeded in the bottom of gels formed into one circularly-shaped mold of 23mm diameter and 300'000 HaCaT cells were seeded in the bottom of gels formed into rectangular molds or on top of gels formed into transwell inserts. Seeding of keratinocytes was made by manual pipetting. Cultivation of the gels, submerged into fibroblast growth medium, followed in a humidified incubator (37 °C, 5% CO<sub>2</sub>) for 3 days, and then the gels were transferred at the state of air-liquid interface for 5 more days of incubation. At the air-liquid interface, keratinocytes differentiation medium was added in such a quantity that only the free of keratinocytes surface of the gel is in contact with it, while the other surface was free of medium. Keratinocytes differentiation medium was replaced every two days.

### 2.3.3. Forming Molds and Cases

The forming molds were used for the generation of skin analogues inside them. The skin constituents were pipetted or injected by the skin-producing machine into the molds and in-mold cultivation followed. The molds were fabricated by attaching micro-porous polyethylene terephthalate (PET) membrane (Unique-Mem® Track-Etched Membranes, Oxyphen) with the use of a soldering iron on both sides of polystyrene rings of 1mm thickness and 23mm diameter or on both sides of polystyrene rectangulars, having three rectangular openings of 1mm thickness and dimensions 23mm x 6mm. One surface of the polystyrene pieces was fully covered by membrane while small holes of about 6mm diameter were left uncovered in the other side to enable insertion of skin constituents.

The polystyrene molds were designed in SolidWorks 2016 and fabricated by laser-cutting. Troctec laser-cutter owned by the Product Development Group at Technopark Campus was used for laser-cutting. After fabrication, the molds were sterilized by immersion into 70% Ethanol for 30 minutes, exposure under UV light into the clean bench for 60 minutes and exposure under Oxygen Plasma at 25% Intensity for 40 minutes (Femto Plasma Cleaner owned by Scope M and operated by Dr. Sung Sik Lee, DIENER ELECTRONICS).

Right before injection, the molds were encased with rectangular plexiglass cases with the guidance of a polystyrene adaptor and with screws. These cases helped to support the molds' membranes and facilitate handling.

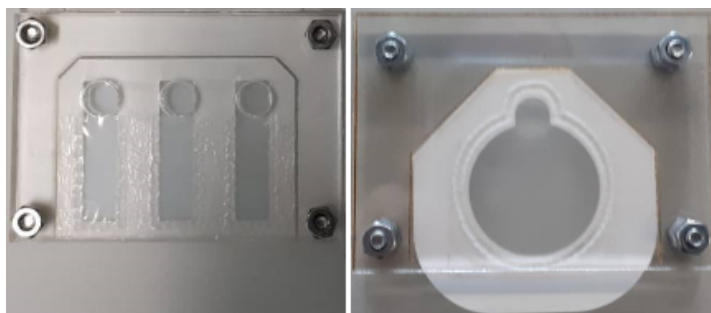


Figure 2.1: Encased polystyrene molds: Mold with rectangular openings in dimensions 23mm x 6mm (left) and circular mold with diameter 23mm (right).

Figure 2.1 illustrates the encased molds. The cases were also designed in SolidWorks 2016 and fabricated by laser-cutting. The cases were cleaned by spraying them with 70% Ethanol and exposing them under UV light into the clean bench for 60 minutes.

### 2.3.4. Air-Liquid Interface Holders

Polystyrene holders were used to lift the molds containing the dermo-epidermal hydrogels at the air-liquid interface to allow keratinocytes to differentiate and form different epidermal layers. They were also designed in SolidWorks 2016 and fabricated by laser-cutting. After fabrication, the holders were sterilized by immersion into 70% Ethanol for 30 minutes, exposure under UV light into the clean bench for 60 minutes and exposure under Oxygen Plasma at 25% Intensity for 40 minutes (Femto Plasma Cleaner owned by Scope M and operated by Dr. Sung Sik Lee, DIENER ELECTRONICS). Prior to use, the different components of the air-liquid holders were manually assembled into the clean bench and exposed again under UV light for 60 minutes. Figure 2.2 illustrates the holders with and without the rectangular mold of 23 mm x 6 mm dimensions.



Figure 2.2: Assembled polystyrene holders used to lift the molds at the air-liquid interface. Assembled holders without the mold (left) and with the mold (right).

## 2.4. Analysing Methods

Biological evaluation of the skin models, which is described in this chapter, took place at the Pharmacogenomics Lab of Professor Detmar at Höggerberg Campus of ETH Zürich with essential guidance by Laboratory Technician Jeanette Scholl, Dr. Carlotta Tacconi and PhD student Jihye Kim.

### 2.4.1. Transwell Migration Assay

The Transwell Migration Assay was performed to examine the migration of HaCaT cells through the pores of the molds' membrane. Pore size of 5 $\mu$ m and 1 $\mu$ m pore were both tested. HaCaT cells were seeded into transwell inserts with 1  $\mu$ m and 5  $\mu$ m pore size in 24 well plates. The transwell inserts were firstly coated with type I collagen (50  $\mu$ g/mL in DPBS, PureCol, Advanced BioMatrix, San Diego, USA) for 20 minutes. Then the collagen solution was removed and 600  $\mu$ L of growth medium was added into the lower chamber, while 100  $\mu$ L of starvation medium (DMEM with 1% FBS and antibiotics) containing HaCaT cells in a concentration of 400,000 cells/mL was added into the upper chamber. After 4 hours of incubation at 37  $^{\circ}$ C and 5% CO<sub>2</sub>, the cells were fixed with 4% Paraformaldehyde (Sigma) for 10 minutes at room temperature. After fixation, the transwell inserts were washed 3 times with DPBS (1x, Gibco). Then, the cells were stained with Hoechst in dilution of 1:1000 in DPBS (1x, Gibco) for 10 min at room temperature in dark. Afterwards, the cells from the upper side of the membrane were removed by cotton swabs. Then, the transwell inserts were washed 3 times with DPBS (1x, Gibco). A scalpel was used to take out the membranes from the inserts and the down-side of membranes, which had the migrating cells, was placed on a drop of Mowiol (Sigma) on a glass slide. The glass slide was then covered with a coverslip. Imaging with a Fluorescent Microscope detected the migration of the HaCaT cells through the membrane.

Four transwell inserts per porosity were examined, while five pictures with 10x Objective

were taken per sample. ImageJ (public domain software, [http:// imagej.nih.gov/ij/](http://imagej.nih.gov/ij/)) was used to quantify the number of migrating cells per pictures and Prism was used for processing the results and generating graphs.

### 2.4.2. Shrinkage Observation

Pictures of the fabricated dermal hydrogels both into transwell inserts and molds were taken right after fabrication as well as one day, seven days and three weeks after fabrication for visual observation of the gels' shrinkage.

### 2.4.3. Fluorescence Microscopy

Dermal gels containing GFP-HDFn were also fabricated both manually in a collagen concentration of 5 mg/mL and automatically in collagen concentrations of 10 mg/mL, 15 mg/mL and 25 mg/mL to detect the viability of the fibroblasts as well as their distribution in the gels of different collagen concentrations. Fluorescent Microscopy (Zeiss Axiovert 200 M microscope, Zeiss AxioCam MRm camera, Carl Zeiss AG, Feldbach, Switzerland) was used for detection. Triplicate of each condition was fabricated and imaged, while three images per sample were taken with 10x objective, one and seven days after fabrication. Processing of the images and measurement of the fluorescent area per image was done with ImageJ to detect the level and consistency of fluorescence, and hence the cells distribution within a single sample as well as between samples of the same collagen concentration or of different collagen concentrations. Prism was used for processing the results and generating graphs.

### 2.4.4. Live-Dead Staining

Viability of the cells into hydrogels of different collagen concentrations was quantified by Live-Dead Staining. The gels were firstly digested by immersing each of them into 1 mL of 4 mg/mL Collagenase type I in fibroblasts growth medium and turning them clockwise, while immersed, for 30 minutes into an incubator at 37°C. After digestion of the hydrogels, centrifugation at 1500rpm for 1 minute followed and the supernatant was discarded. The samples were washed with DPBS (1x, Gibco) and then centrifuged again at 1500rpm for 1 minute. The samples were stained with Zombi NIR APC cy7 in DPBS (1x, Gibco) in dilution 1:4000. After 15 minutes at room temperature, the samples were washed with FACS Buffer (Phosphate-Buffer Saline, 1mM EDTA, 2% Fetal Bovine Serum) and centrifuged at 1000rpm for 5 minutes. The supernatant was discarded, and the samples were fixed with 1% Paraformaldehyde.

Fluorescence-activated cell sorting (FACS) was employed for the discrimination between alive and dead cells, and FlowJo was used for processing the results and generating graphs. Positive and negative controls were also used for validation of the experiment. Zombi NIR APC cy7 stained the dead cells, so the negative control included 200,000 alive fibroblasts, derived directly from 2D cultures, while the positive control included 200,000 fibroblasts, derived directly from 2D cultures and treated with 90% Dimethyl Sulfoxide (DMSO) to kill the cells. Gating of the alive cell population was chosen in the generation of the graphs.

### 2.4.5. Histology

At the time point of interest, the skin hydrogels were fixed with 4% Paraformaldehyde at room temperature for two hours in dark condition. Then, the hydrogels were stored in 70% Ethanol at 4°C until further processing. At time of processing, the samples were transferred into 70% Ethanol at room temperature for 60 minutes, then they were immersed into 90% Ethanol for 30 minutes and into 100% Ethanol for 60 more minutes, while afterwards they were immersed in Xylene, for three times of 20 minutes each. Immersion in liquid paraffin at 60°C followed for 4-6 hours before the samples were embedded into paraffin. Polymerization needed 30 minutes to happen and then the embedded samples were stored at 4°C until sections of 5µm were taken. Sections were permanently placed on top of glass slides and labeled accordingly, while they were stored at 4°C until further processing.

Prior to the desired staining, baking of the sections at 65°C for one hour and deparaffinization of the sections (3 times for 5 minutes each in Xylene, 2 times for 2 minutes each in

100% Ethanol, 1 time for 2 minutes in 95% Ethanol, 1 time for 2 minutes in 90% Ethanol, 1 time for 2 minutes in 80% Ethanol, 1 time for 2 minutes in 70% Ethanol, 1 time for 2 minutes in 50% Ethanol, 1 time for 3 minutes in Phosphate Buffered Saline(1X, Gibco), 1 time for 5 minutes in Distilled Water) took place.

#### 2.4.5.1. Haematoxylin & Eosin Staining

Haematoxylin and Eosin Staining is the most common staining method in histology, used for demonstration of nucleus (red colour) and cytoplasm (pink colour). In this master thesis, it was applied on fixed dermal samples and dermo-epidermal hydrogels and was used to illustrate the morphology of the dermal and epidermal layers, as well as the differentiation of keratinocytes.

The process included firstly immersion of deparaffinized and rehydrated sections into tap water for a few minutes before immersion into Haematoxylin Solution for 3 minutes to stain the nuclei. Then, the sections were immersed into tap water for 30 seconds, into acid ethanol (HCL-EtOH solution) for a few seconds for slight de-staining, into tap water for 1 minute, into Eosin Solution for 1 minute to stain the cytoplasm and again into tap water for 1 minute. Dehydration followed by immersion of the stained slides into 100% Ethanol for 2 times of 30 seconds each and then into Xylene for 2 times of 1 minute each. Finally, the sections were mounted with two drops of Eukitt Quick-Hardening Mounting Medium (100mL, Sigma-Aldrich) on each glass slide and then covered with cover-slips carefully so that no bubbles were formed. After letting the slides dry in the hood for one hour or more, imaging took place with a Microscope and figures in 10x magnification were taken.

#### 2.4.5.2. Herovici Staining

Herovici Staining included picro methyl blue or aniline blue and picro acid fuchsin in proper proportion, dyeing the mature dense collagen with red colour, the reticulum and newly formed collagen with blue colour and the cytoplasm with yellow colour [58]. In this master thesis, Herovici staining was employed to demonstrate the potential remodelling of the dermal hydrogels by the embedded fibroblasts. It was applied on dermal hydrogels, fixed one and three weeks after fabrication.

For the Herovici staining, the Herovici's Collagen Stain Kit (American MasterTech) was employed. The kit included Herovici's Stain Solution A, Herovici's Stain Solution B, Weigert's Haematoxylin A, Weigert's Haematoxylin B and 1% Acetic Acid. Exactly before use, Weigert's Haematoxylin A and Weigert's Haematoxylin B were mixed, and the same applies to the Herovici's Stain Solution A and Herovici's Stain Solution B. The implemented process was based on the guidelines given by American MasterTech, and therefore a deparaffinizing and rehydration process, slightly different from the one mentioned in section 2.4.5, was followed.

After baking the 5µm sections at 65 °C, they were immersed in Xylene for 2 times of 5 minutes each. Then, they were rehydrated by rinsing them with 100% Ethanol for 3 times of 1 minute each. Washing with running tap water for 1 minute followed. The sections were immersed into Weigert's Haematoxylin Solution for 5 minutes, and then were rinsed with tap water for 1 minute. Immersion into Herovici's Working Solution for 2 minutes and then into 1% Acetic Acid for 1 minute follow. Dehydration took place by immersing the sections into 100% Ethanol for 3 times of 1 minute each, and then into Xylene for 3 times of 1 minute each. Finally, the sections were mounted with two drops of Eukitt Quick-Hardening Mounting Medium (100mL, Sigma-Aldrich) on each glass slide and then covering with cover-slips, carefully so that no bubbles were formed. After letting the slides dry in the hood for one hour or more, imaging took place with a Microscope.

#### 2.4.5.3. Immunofluorescence

Immunofluorescence is a technique employing antibodies to correspond fluorescent dyes to particular biomolecule targets. In this master thesis, it was applied on fixed dermo-epidermal hydrogels to detect keratinocytes marker cytokeratin10, as well as cells' nuclei. Hoechst dye was employed in dilution 1:1000, at the same time point as the secondary antibodies, in order to dye cells' nuclei in fluorescent blue colour. Cytokeratin 10 is marker for keratinized stratified epithelium and hence, it was used to detect the differentiation of keratinocytes

in dilution 1:200. Donkey Immunomix Blocking Buffer (0.2% Bovine Serum Albumin, 5% Donkey Serum, 0.05% Sodium Azide ( $\text{NaN}_3$ ) and 0.3% Triton X-100 in Phosphate Buffer Solution) was used to dilute the antibodies. Secondary antibody S22 was used in dilution 1:200 to dye cytokeratin 10 with green colour.

After the deparaffinization and rehydration process mentioned in section 2.4.5, the slides were moved from distilled water into freshly made antigen retrieval (0.1M Trisodium Citrate, 0.1M Citric Acid and distilled water) to eliminate any paraformaldehyde-caused chemical modifications that reduce proteins' detectability. While immersed into the antigen retrieval, the slides were firstly placed in water bath of 60°C for 20 minutes, and then at room temperature for 20 minutes. Later, the slides were rinsed with Tris-buffered saline containing 0.1% Triton-X for 3 times of 5 minutes each. A blocking pen was used to mark the area of the slides that had to be stained, and then Donkey Immunomix Blocking Buffer (0.2% Bovine Serum Albumin, 5% Donkey Serum, 0.05% Sodium Azide ( $\text{NaN}_3$ ) and 0.3% Triton X-100 in Phosphate Buffer Solution) was applied for 1 hour at room temperature. Later, the slides were rinsed with Tris-buffered saline containing 0.1% Triton-X for 5 minutes, and the primary antibodies were added. Overnight incubation at 4°C followed. The next day the slides were rinsed 3 times for 5 minutes each with PBS, and then the secondary antibodies were applied for 30 minutes at room temperature with dark condition. After 30 minutes the slides were rinsed for 3 times of 5 minutes each with PBS at room temperature and then with distilled water for 2 times of 5 minutes each. Finally, the slides were mounted with two drops of Mowiol Mounting Medium and then covered with cover-slips carefully so that no bubbles were formed. After letting the slides dry in the hood for one hour or more, imaging took place with a Fluorescent Microscope, and figures in 10x magnification were taken.

#### **2.4.6. Statistical Analysis**

Unpaired two-tailed t-test was utilized to compare migration of keratinocytes through different membrane porosities and repeated measures ANOVA was implemented to compare the fluorescent area within and between dermal hydrogels containing GFP-HDFn. Data were expressed as mean & standard error of mean, and differences were considered statistically significant when  $p < 0.05$ . Prism was utilized for the conduction of the statistical analysis.



# 3

## Results

### 3.1. Mold Design Effect on Dermal Hydrogels

The Pharmacogenomics lab utilizes transwell inserts for the manual generation of skin models while as the name of the process reveals, molds are used for the automated injection molding of skin equivalents. The transwell inserts as well as two different mold designs were compared in this study in terms of hydrogels shrinking, within and between hydrogels homogeneity, ease of manipulation during analytical processing, as well as successful generation of the epidermal layer.

#### 3.1.1. Flaws of Transwell Inserts

The first experiments included a general comparison between the two different methods: manual fabrication of dermal hydrogels of 5mg/mL collagen concentration into 12 mm transwell inserts with 0.4 $\mu$ m pore polyester membrane inserts and automated injection of 25mg/mL collagen concentrated dermal hydrogels into circular molds of 23mm diameter. During these experiments, it was detected that many skin hydrogels fabricated into the transwell inserts do not have homogeneous thickness (Figure 3.1A) while they are also shrinking during the cultivation period (Figure 3.1B). Besides, throughout the paraffinizing process they are shrinking more, and some of them cannot be eventually subjected to histological evaluation and screening (Figures 3.1C and 3.1D).



Figure 3.1: Dermal hydrogel with inhomogeneous thickness one day after fabrication (A). Shrunken dermal hydrogel one week after fabrication (B). Dermal hydrogel before (C) and after the paraffinizing process (D).

#### 3.1.2. Effect of Shape and Size of Molds on Dermal Hydrogels

##### 3.1.2.1. Circular Mold of 23mm Diameter

In contrast to the low-concentrated hydrogels into transwell inserts, skin hydrogels fabricated into circular molds of 23mm diameter by automated injection molding maintain their shape and size during the whole cultivation period and during analytical processing while they have homogeneous thickness which is defined by the mold. Such a dermal hydrogel can be seen in the Figure 3.2, which is retrieved by the master thesis of Jessica Polak <sup>[59]</sup>. The theoretical

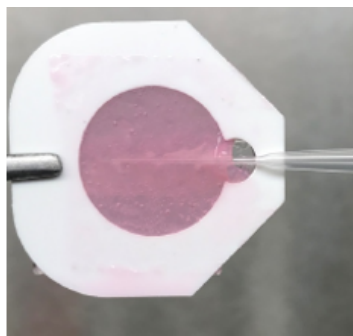


Figure 3.2: Seeding of keratinocytes in circular dermal hydrogel of 23mm diameter (Figure retrieved by master thesis of Jessica Polak<sup>[59]</sup>) Pink colour of the hydrogels results from the fibroblasts growth medium.



Figure 3.3: Half part of 23mm diameter hydrogel exceeds the molds dimensions (left) and it is further cut in two pieces (right).

volume of skin mixture required to fill this mold is  $416\mu\text{L}$ , and the actually pipetted or injected is 1ml. This means that used fibroblasts number is about five times more than in case of one 12 mm transwell insert.

Also, the diameter of 23mm is a restraining factor for the seeding of keratinocytes, as well as for the embedding process. As it can be observed in Figure 3.2, the wide surface of the hydrogels demands several times of pipetting in different angles to generate an epidermal layer on the whole surface with potential overlapping during the pipetting process or it demands removal of the membrane prior to the seeding. Besides, as illustrated in Figure 3.3, even the half part of a 23mm diameter hydrogel exceeds the height of the embedding mold and the hydrogel is cut in four pieces before embedding.

### 3.1.2.2. Mold with Triplicate of Rectangular Inserts

Based on the above results, another mold was generated. Figure 3.4 compares the dimensions of the two different mold types. This new mold forms three hydrogels of 6mm width and 23mm length, which conform to the dimensions of the embedding mold, as depicted in Figure 3.5. A triplicate of rectangular hydrogels may be embedded in a single mold, while as illustrated in the right part of Figure 3.5, this width allows seeding of keratinocytes in a single direction.

Additionally, the new mold contains three inserts for the formation of triplicate dermal hydrogels, each of which demands about three times less volume than the bigger mold (theoretical filling volume is  $138\mu\text{L}$  and practically  $400\mu\text{L}$  are injected or pipetted), which is translated to three times less fibroblasts, as well. Differences are observed in the degree of size maintenance of the hydrogels between transwell inserts and rectangularly-shaped molds. Molds preserve the shape of the hydrogels throughout the whole cultivation period, even in case of low collagen concentrated hydrogels. Figure 3.6 depicts dermal hydrogels of 5mg/mL collagen concentration manually generated into a 12mm transwell and into a rectangular mold after three weeks of cultivation. In this figure, shrinkage is observed in case of the transwell insert.

In case of low-concentrated collagen hydrogels (i.e. 5mg/mL), if a volume of about  $150\mu\text{l}$  is pipetted into each insert of the mold, the hydrogels' shrinkage occurring during the 30 minutes of curing period into the incubator ( $37^\circ\text{C}$ , 5%  $\text{CO}_2$ ) due to evaporation, results in

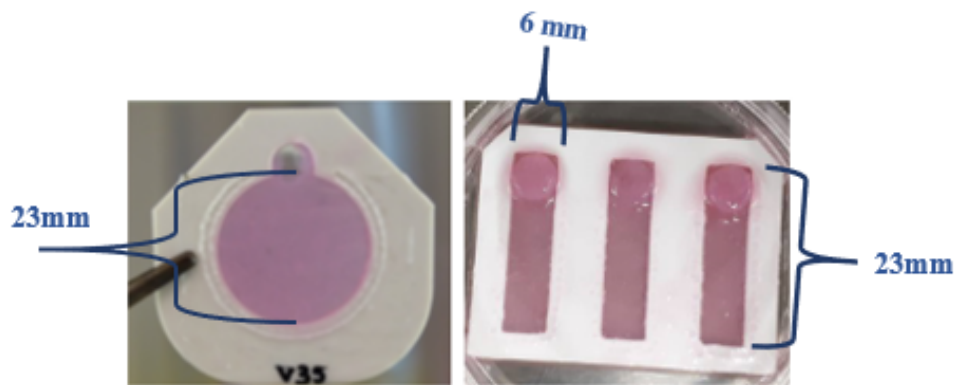


Figure 3.4: Skin models into the two types of polystyrene molds: circular mold of 23mm diameter (left), and rectangular forming mold for 3 hydrogels in dimensions 23mm x 6mm (right). Hydrogels have pink colour thanks to the fibroblasts growth medium.

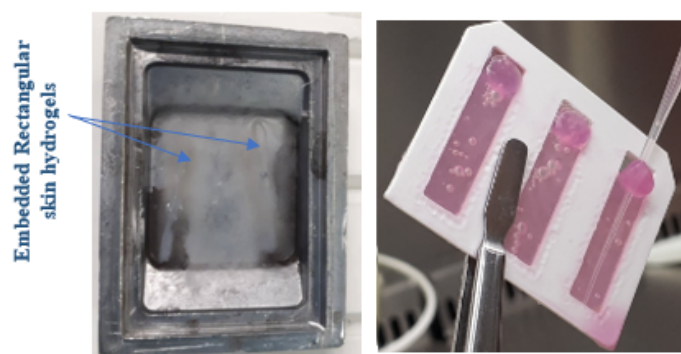


Figure 3.5: Two hydrogels (indicated by blue arrows) embedded in the same embedding mold (left). Single directional seeding of keratinocytes in dermal hydrogels formed into the rectangular mold (right).

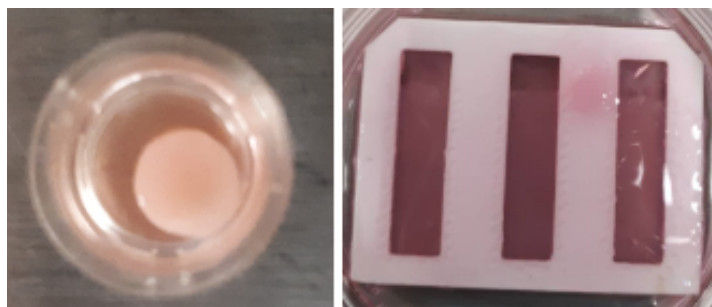


Figure 3.6: Shrunken dermal hydrogel into a 12mm transwell (left) and dermal hydrogels with maintained size into the rectangular mold (right). Low-concentrated collagen and manual fabrication were utilized in both cases and cultivation lasted 3 weeks.



Figure 3.7: Low-concentrated (5mg/mL) collagen hydrogels at the moment of formation (left) and after 30 minutes of incubation (right), during which a small amount of the volume is evaporated affecting the final size of the hydrogels.

smaller hydrogels as it can be seen in Figure 3.7. When 400 $\mu$ L are pipetted, they also fill the case holes and evaporation does not affect the size of the hydrogels, as it is seen in right part of Figure 3.6.

### 3.1.2.3. Automated Injection into Molds

As mentioned in section 2.3.2. during the automated injection molding the encased molds are positioned on a base to eliminate manual holding. More specifically, the circular molds of 23mm diameter are placed on top of an inclined base, which can be seen in the upper part of Figure 3.8<sup>[52]</sup>. Utilization of this base during the injection molding into rectangularly-shaped molds resulted in incomplete filling of the molds, as illustrated in the left part of Figure 3.9. Trials of injection into rectangularly-shaped molds while positioned in different inclinations resulted eventually in the generation of fully flat base, which ensures complete filling of these molds, as depicted in the right part of Figure 3.9 This base can be seen in the lower part of Figure 3.8 and was constructed by the same materials and fabrication method as the inclined one.

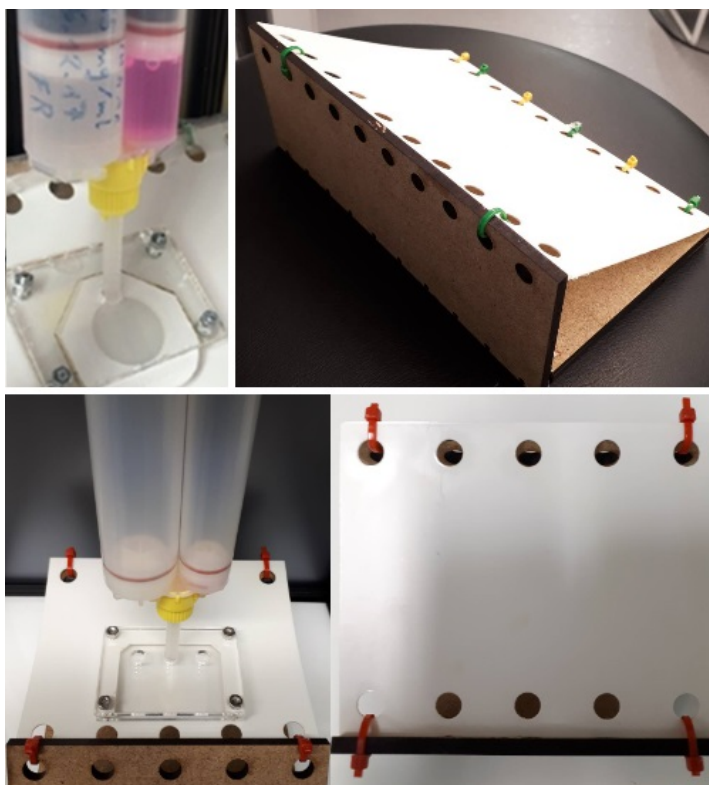


Figure 3.8: Inclined base used for positioning the encased circularly shaped molds during automatic injection molding (up<sup>[52]</sup>), and flat base used for positioning the encased rectangularly-shaped molds during injection (down).

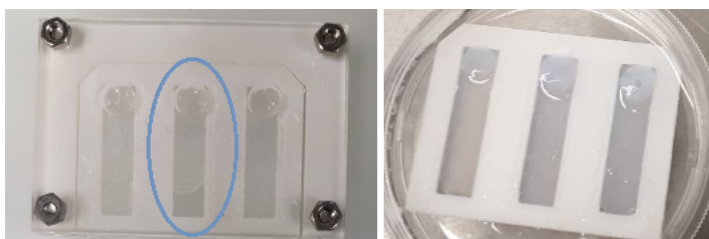


Figure 3.9: One of the three hydrogels of 25mg/mL collagen concentration formed by automated injection molding into rectangular molds is not fully filled with the dermis constituents when the inclined base is utilized (left) while completely filled mold occurs when flat base is used (right).

### 3.1.3. Effects of Membrane Pore Size on Keratinocytes Migration

The membrane of the 23mm diameter molds used in the first experiments of this master thesis had pore size of  $5\mu\text{m}$ . Histological evaluation, specifically Haematoxylin & Eosin Staining, showed that keratinocytes can migrate through these pores and form an epidermal layer above the membrane, as it can be seen in Figure 3.10.

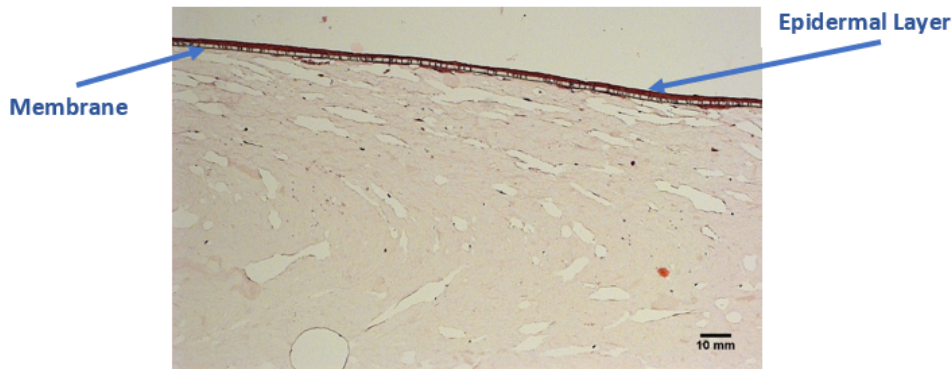


Figure 3.10: Haematoxylin & Eosin Staining on  $5\mu\text{m}$  section of a dermo-epidermal hydrogel. Epidermal layer (Layer of deep red colour indicated by blue arrow) is formed above the membrane of  $5\mu\text{m}$  pore size (white layer indicated also by blue arrow).

Implementation of transwell migration assay further supported that some keratinocytes are migrating through this pore size. After 4 hours into transwell inserts with pore size of  $5\mu\text{m}$ , a mean number of 18 keratinocytes with a standard error of 2.16 migrated through the membrane's pores of four transwell inserts in total (sample size,  $N=4$ ). In case of  $1\mu\text{m}$  pore size, a mean number of 3 migrating keratinocytes with a standard error of 0.58 was detected, which is 6 times smaller than in the case of  $5\mu\text{m}$  pore size. The p-value of the unpaired two-tailed t-test implemented for these two populations was calculated to be 0.00053 which is considered as statistically significant. Figure 3.11 portrays a bar graph presenting the keratinocytes migration.

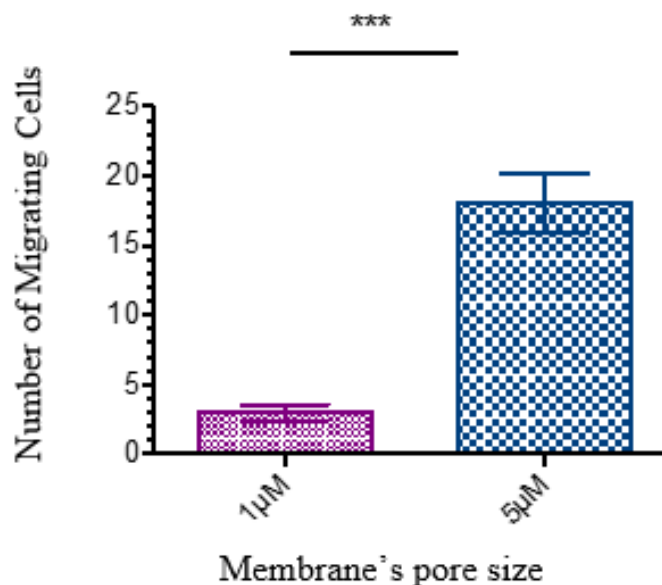


Figure 3.11: Bar graph showing the number of migrating keratinocytes 4 hours after their seeding in case of two membranes with different pore size ( $N=4$ ). An average number of 3 cells with standard error of 0.58 migrated through the membrane of  $1\mu\text{m}$  pore size and an average number of 18 cells with standard error of 2.16 migrated through the membrane of  $5\mu\text{m}$  pore size. The difference between the two samples was found statistically significant with a p value of 0.00053.

## 3.2. Collagen Concentration Effect

Traditional manual production of skin hydrogels into the transwell inserts includes low concentration collagen (i.e. 5mg/mL), while the automated injection molding method had only been tested in the generation of skin hydrogels of 25mg/mL collagen concentration. These two concentrations, as well as two intermediate collagen concentrations (i.e. 10mg/mL and 15mg/mL) for which also automated injection molding was employed, were compared in this study in terms of fibroblasts' viability, distribution in the dermal matrix, collagen remodelling by fibroblasts, keratinocytes viability and differentiation, as well as in terms of hydrogels stability, homogeneity and shape and size maintenance, as well as in terms of ease of manipulation during analytical processing.

### 3.2.1. Shrinkage of Hydrogels

Skin hydrogels of different collagen concentrations were fabricated both into molds and into transwell inserts. For the 5mg/mL collagen concentration manual method was employed while for all the other concentrations automated injection molding was utilized. In-mold hydrogels maintained their size throughout the whole cultivation period regardless of the collagen concentration, as Figure 3.12 shows. Also, skin hydrogels of 10mg/mL, 15mg/mL and 25mg/mL collagen concentration formed into transwell inserts maintained their size in contrast to low-concentrated collagen hydrogels, as Figure 3.13 reveals. Inconsistencies in thickness is observed when transwell inserts are used regardless of the fabrication process or the collagen concentration.

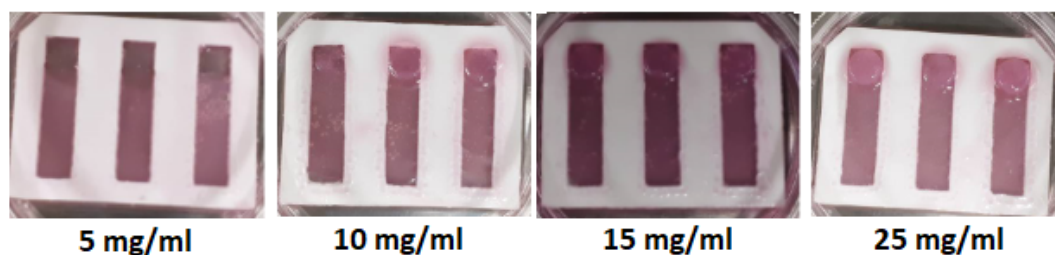


Figure 3.12: In-mold dermal hydrogels of different collagen concentrations do not suffer from shrinkage one week after fabrication.

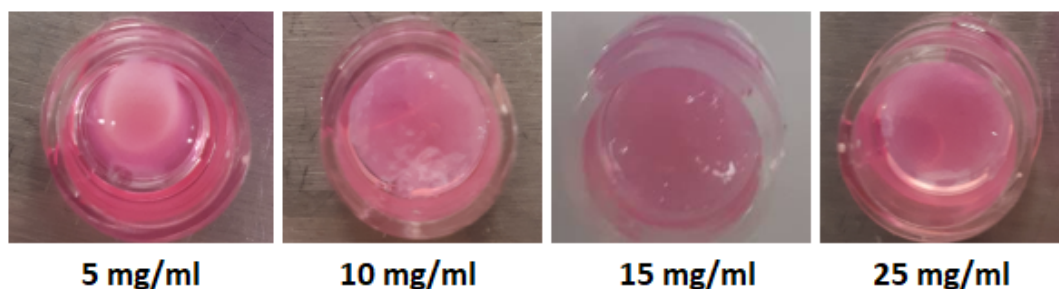


Figure 3.13: Dermal hydrogels of different collagen concentrations into transwell inserts. Manually produced hydrogel of 5mg/mL collagen concentrations shrunk and has smaller diameter while the rest hydrogels, fabricated by automated injection molding, maintained their initial diameter one week after fabrication.

### 3.2.2. Fibroblasts Viability

The results of live-dead staining are summarized in Figure 3.14. Positive control which represents killed cells was used to support the reliability of the experiment, while negative control, which represents fibroblasts directly derived from 2D culture, served as benchmark to help characterize the experiments' results. Dermal hydrogels of 5mg/mL collagen concentration expressed the highest fibroblasts viability of about 90%, only 3% less than the negative control. Manually and automatically produced dermal hydrogels of 5mg/mL concentration

expressed similar viability. Dermal hydrogels of 10mg/mL and 15mg/mL collagen concentration exhibited a viability of approximately 77% while the highest collagen concentration (25mg/mL) resulted in viability of less than 60%. As three samples were tested per case, the histogram of Figure 3.15 illustrates variations in viability between the three different samples of the same collagen concentration. Minimum deviations can be observed between dermal hydrogels of 10mg/mL and 15mg/mL collagen concentration, while significant deviations between the three samples of 5mg/mL and 25mg/mL collagen concentrations can be seen.

### 3.2.3. Fibroblasts Distribution

Fluorescent Microscopy on dermal hydrogels containing GFP-HDFn explored the homogeneity of fibroblasts distribution into the hydrogels. Figures 3.16 and 3.17 are paradigms of fluorescent images of hydrogels of the different collagen concentration, one and seven days after fabrication while Figures 3.18 and 3.19 portray bar graphs of the fibroblasts' distribution between hydrogels of the same collagen concentration as well as between hydrogels of different collagen concentrations one and seven days after fabrication. Each bar depicts also the standard error of mean regarding the cells' distribution within individual hydrogels. Repeated Measures ANOVA resulted in non-significant difference in fibroblasts distribution within and between all the different samples and conditions.

### 3.2.4. Collagen Remodeling

Herovici staining showed that one week old dermal hydrogels of 10mg/mL, 15mg/mL and 25mg/mL collagen concentration and automatically produced, mostly contain mature collagen (reddish purple colour) and scanty freshly-made collagen (blue colour) while plenty freshly-made collagen can be observed in dermal hydrogels of 10mg/mL and 15mg/mL collagen concentration that are three weeks old. 25mg/mL concentrated dermal hydrogels contained both mature and immature collagen after three weeks of cultivation. Figure 3.20 illustrates these findings. Herovici staining failed to detect any type of collagen in manually produced 5mg/mL collagen concentrated dermal hydrogels.

### 3.2.5. Keratinocytes Viability and Differentiation

Keratinocytes viability and differentiation are observed in the Haematoxylin & Eosin stained as well as the immunofluorescent figures presented below. Dermo-epidermal hydrogels of all different collagen concentrations, fabricated into both rectangular molds and transwell inserts by both processes, were successfully stained and a similar morphology of both skin layers can be observed between them. Figure 3.21 illustrates Haematoxylin & Eosin stained hydrogels. In higher concentrations than 5mg/mL, the collagen fibers of dermis are visible in the Haematoxylin & Eosin stained images, while an epidermis of similar thickness is visible in all different hydrogels regardless of the collagen concentration, the formation insert (molds or transwell inserts) or the fabrication method. Immunofluorescent stained hydrogels are viewed in Figure 3.22. All images similarly combine cells nuclei in blue colour and cytokeratin 10 in green colour.

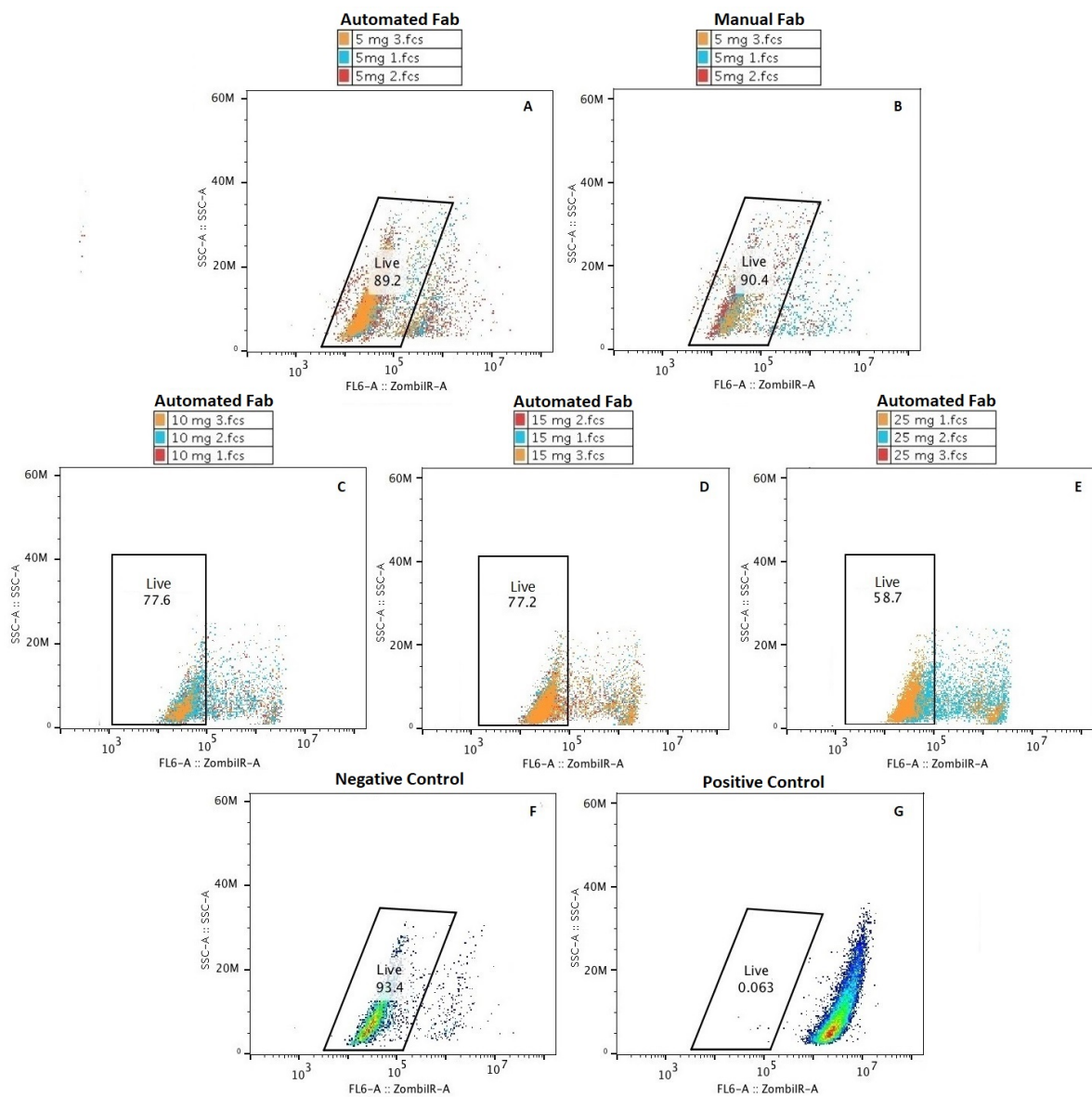


Figure 3.14: Percentage of alive fibroblasts into hydrogels of different collagen concentrations depicted in flow cytometry graphs: Y-axis represents the granularity of the cells and X-axis defines which cells are stained by Zombie NIR (scattered cells) and which are not (non-scattered population). Gating surrounds the alive (non-stained) cells. 89.2% of fibroblasts is alive in case of 5mg/mL concentrated dermal hydrogels produced automatically (A). 90.4% of fibroblasts is alive in case of 5mg/mL concentrated dermal hydrogels produced manually (B). 77.6% of fibroblasts is alive in case of 10mg/mL concentrated dermal hydrogels produced automatically (C). 77.6% of fibroblasts is alive in case of 15mg/mL concentrated dermal hydrogels produced automatically (D). 58.7% of fibroblasts is alive in case of 25mg/mL concentrated dermal hydrogels produced automatically (E). 93.4% of 200'000 dermal fibroblasts derived directly from culture (negative control) is alive (F). All dermal fibroblasts derived directly from culture and treated with 90% DMSO to be killed (positive control) are dead (G).

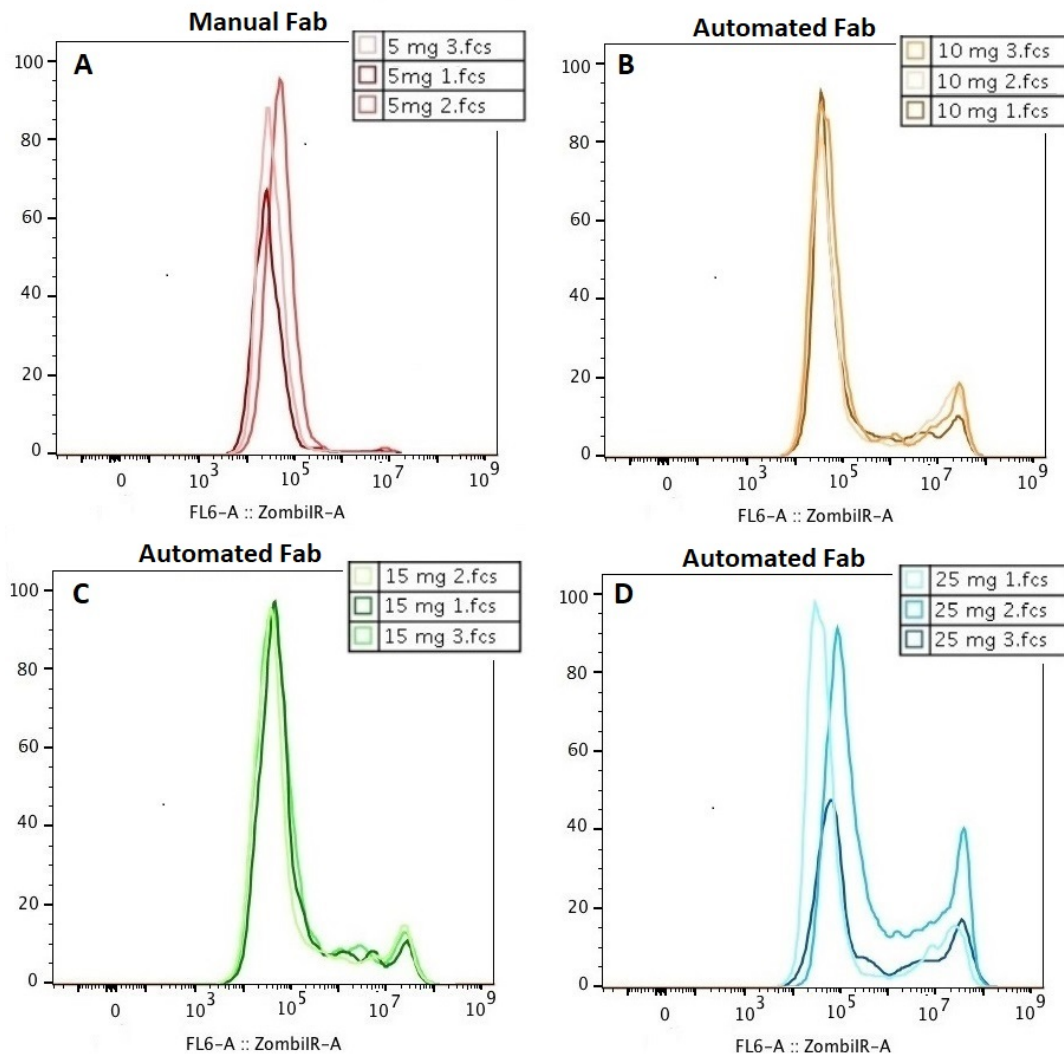


Figure 3.15: Normalized to mode histograms depict variations in viability of fibroblasts into three gels of the same collagen concentration: 5mg/mL – manual fabrication (A), 10mg/mL – automated fabrication (B), 15mg/mL – automated fabrication (C), 25mg/mL – automated fabrication (D).

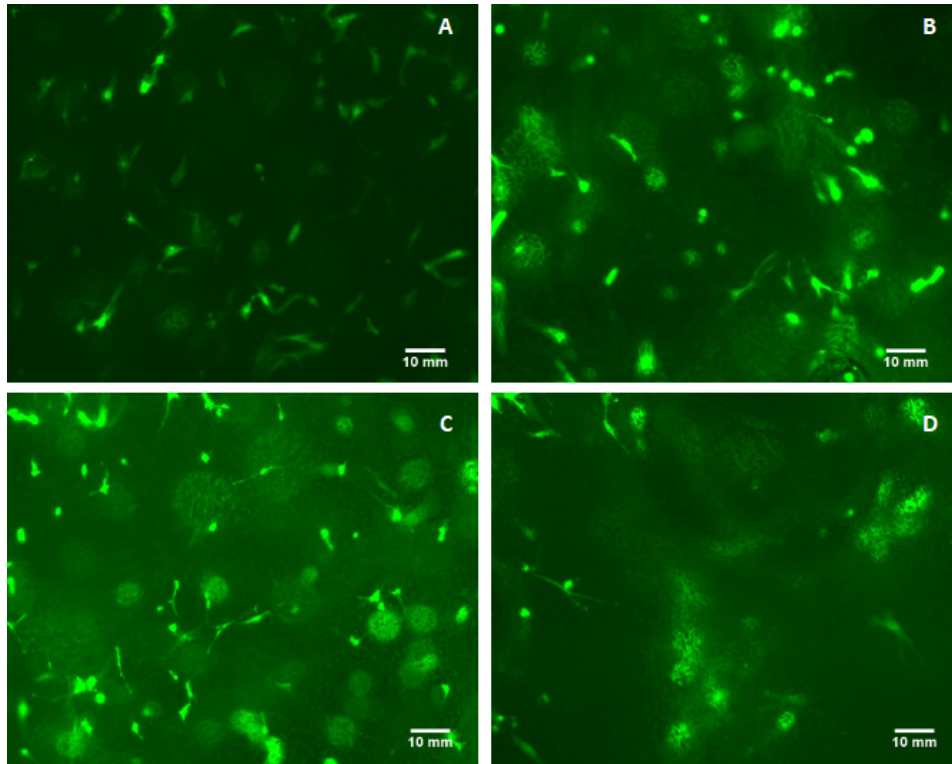


Figure 3.16: Fluorescent images of dermal hydrogels consisting of GFP-HDFn one day after fabrication. 5mg/mL collagen concentration – manual fabrication (A), 10mg/mL collagen concentration – automated fabrication (B), 15mg/mL collagen concentration – automated fabrication (C), and 25mg/mL collagen concentration – automated fabrication(D).

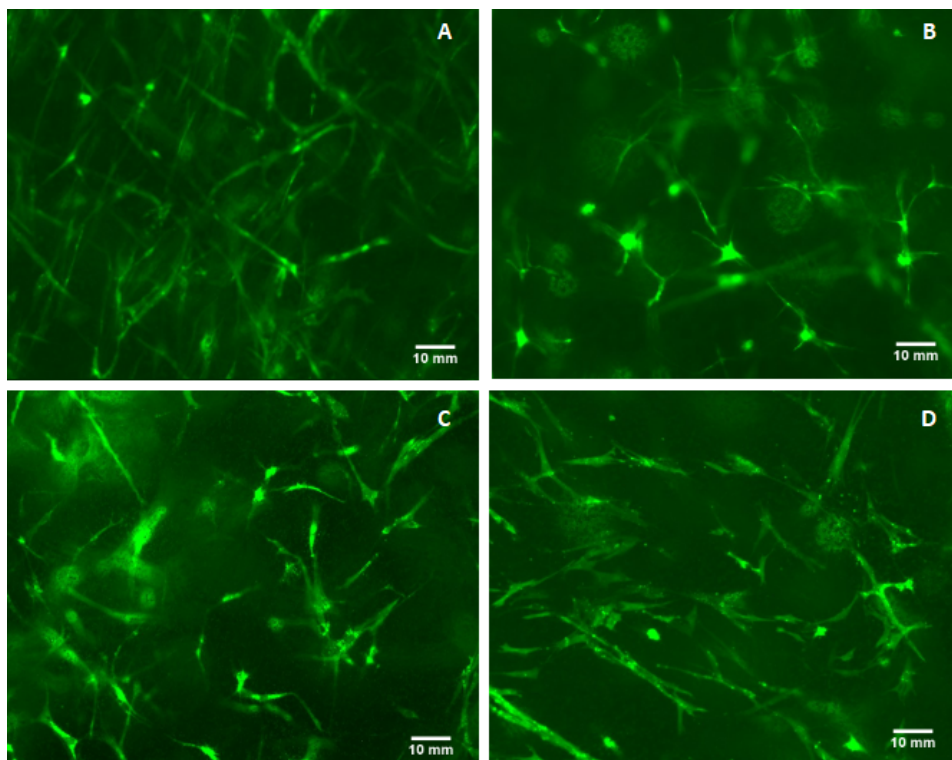


Figure 3.17: Fluorescent images of dermal hydrogels consisting of GFP-HDFn seven days after fabrication. 5mg/mL collagen concentration – manual fabrication (A), 10mg/mL collagen concentration – automated fabrication (B), 15mg/mL collagen concentration – automated fabrication (C), and 25mg/mL collagen concentration – automated fabrication(D).

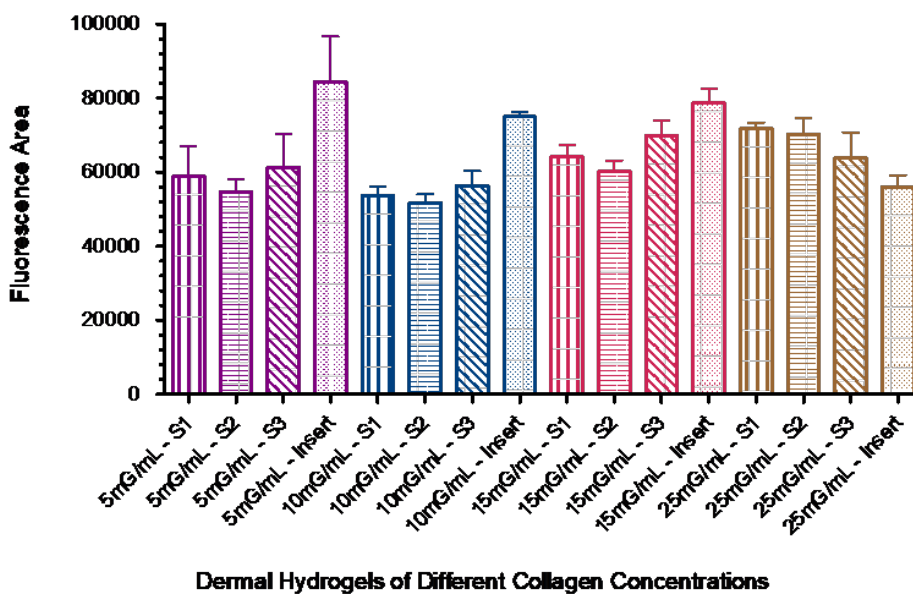


Figure 3.18: Bar graph comparing the fluorescence area between three dermal hydrogels of a single mold and one hydrogel of one transwell insert of the same collagen concentration for all the different concentrations, one day after fabrication of the hydrogels.

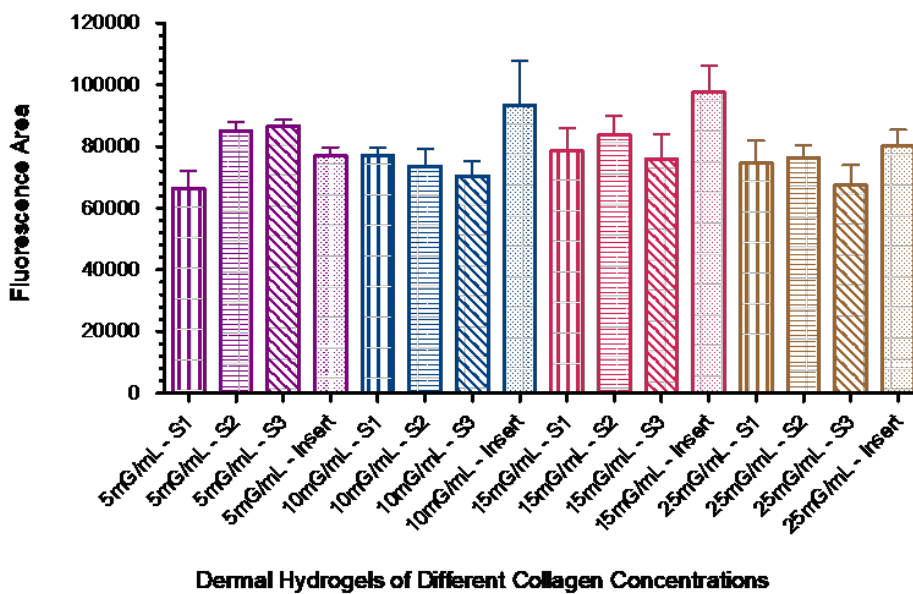


Figure 3.19: Bar graph comparing the fluorescence area between three dermal hydrogels of a single mold and one hydrogel of one transwell insert of the same collagen concentration for all the different concentrations, seven days after fabrication of the hydrogels.

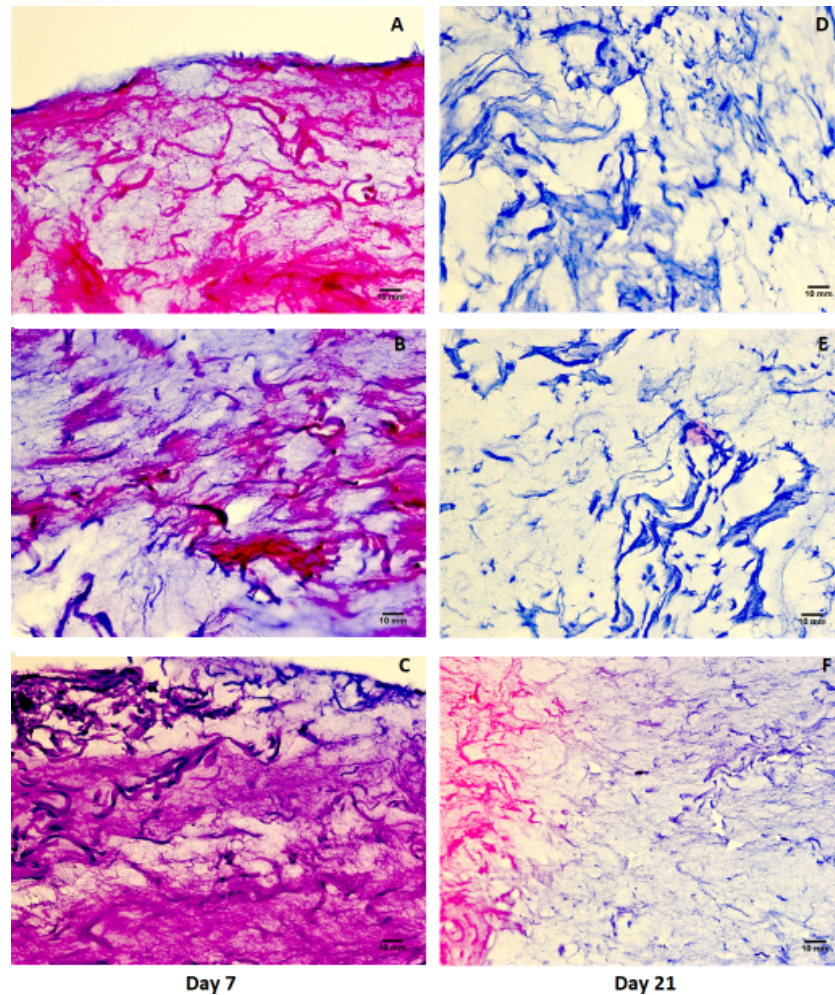


Figure 3.20: Herovici staining on automatically produced dermal hydrogels of 10mg/mL (A), 15mg/mL (B) and 25mg/mL (C) collagen concentration, one and three weeks after fabrication reveals remodelling of the dermal matrix by embedded fibroblasts. Reddish purple colour represents mature collagen and blue colour dyes newly formed collagen. Reddish purple colour is dominant in one week old dermal hydrogels while some blue colour can be also detected. Blue colour dominates in three weeks old dermal hydrogels of 10mg/mL and 15mg/mL collagen concentration, while both colours are observed in 25mg/mL collagen-concentrated hydrogels.

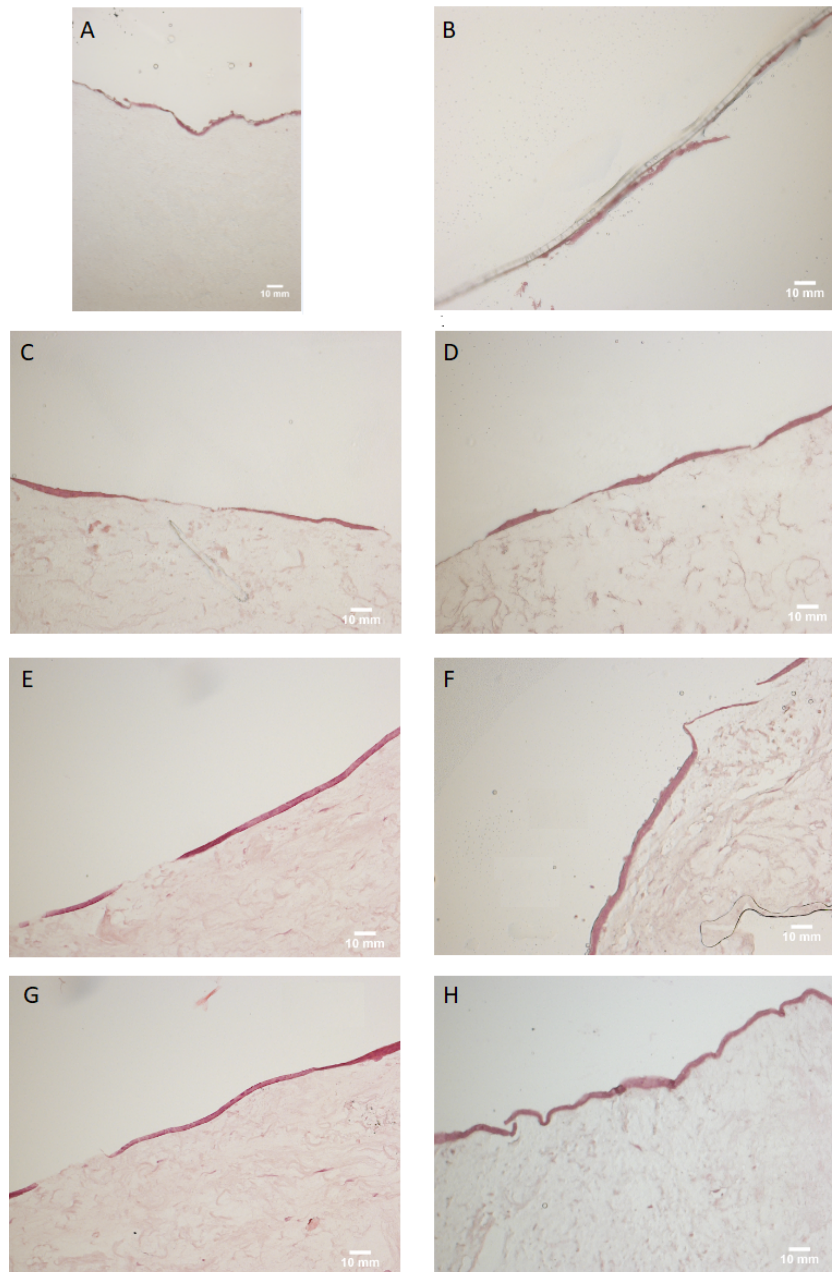


Figure 3.21: Haematoxylin & Eosin Staining of dermo-epidermal hydrogels of different concentrations (A&B: 5mg/mL – manual fabrication, C&D: 10mg/mL – automated fabrication, E&F: 15mg/mL - automated fabrication, G&H: 25mg/mL - automated fabrication) formed into transwell inserts (A, C, E, G) and molds (B,D,F,H). The dense red layer represents the epidermal layer.

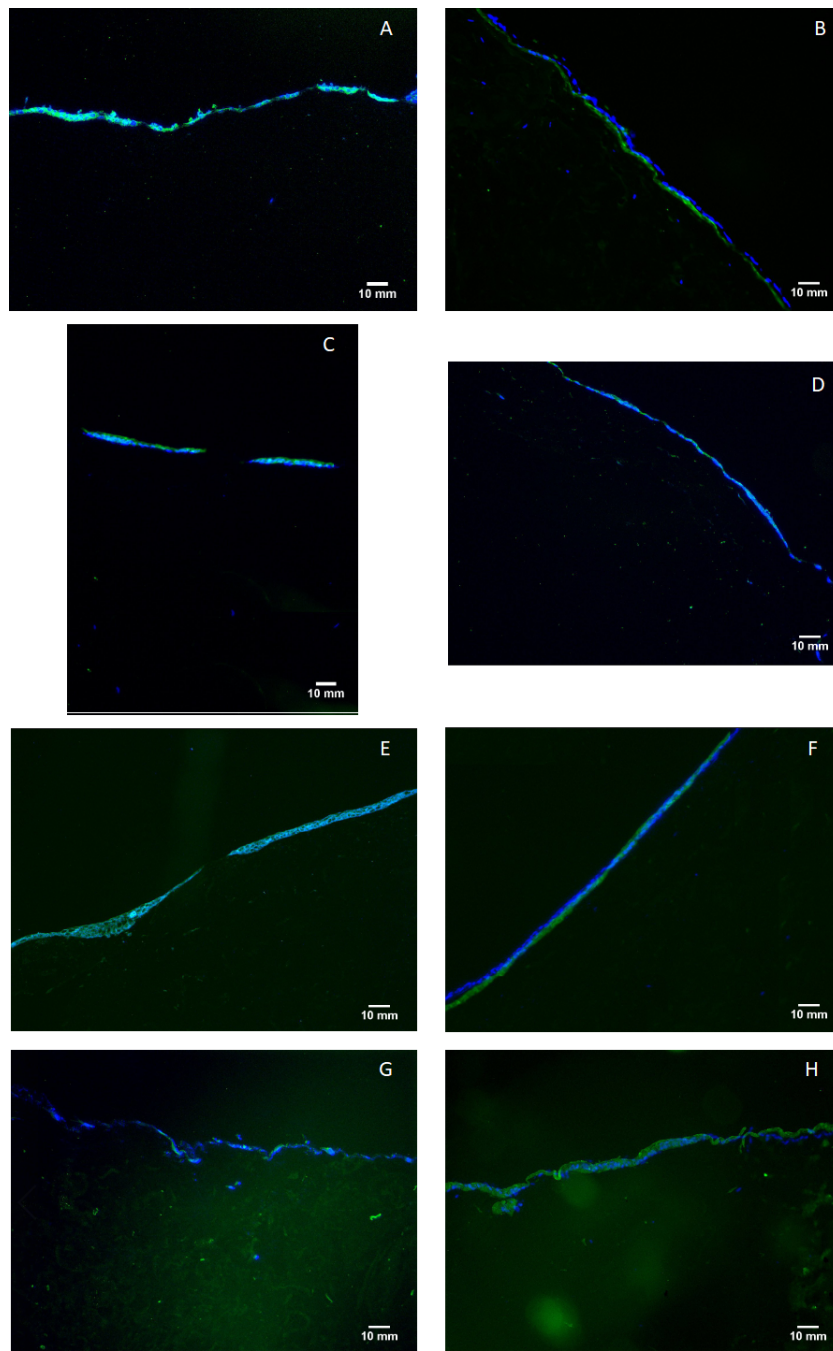


Figure 3.22: Immunofluorescent images of dermo-epidermal hydrogels of different concentrations (A&B: 5mg/mL – manual fabrication, C&D: 10mg/mL – automated fabrication, E&F: 15mg/mL – automated fabrication, G&H: 25mg/mL - automated fabrication) formed into transwell inserts (A, C, E, G) and molds (B,D,F,H) depicting the epidermal layer. The images are composites, with blue colour representing cells nuclei and green colour representing cyokeratin 10, a marker for stratified keratinocytes.

### 3.3. Psoriatic Skin Model

Psoriatic fibroblasts were embedded in collagen hydrogels of 5mg/mL, 10mg/mL and 15mg/mL collagen concentration, formed into rectangular molds. Figure 3.23 illustrates Haematoxylin & Eosin stained dermo-epidermal hydrogels, as well as, immunofluorescent stained hydrogels in which cytokeratin 10 has green fluorescent colour and cells nuclei have fluorescent blue colour. All psoriatic hydrogels included differentiated keratinocytes, while the epidermal thickness in case of 15mg/mL collagen concentrations appear to be slightly thicker in some spots.

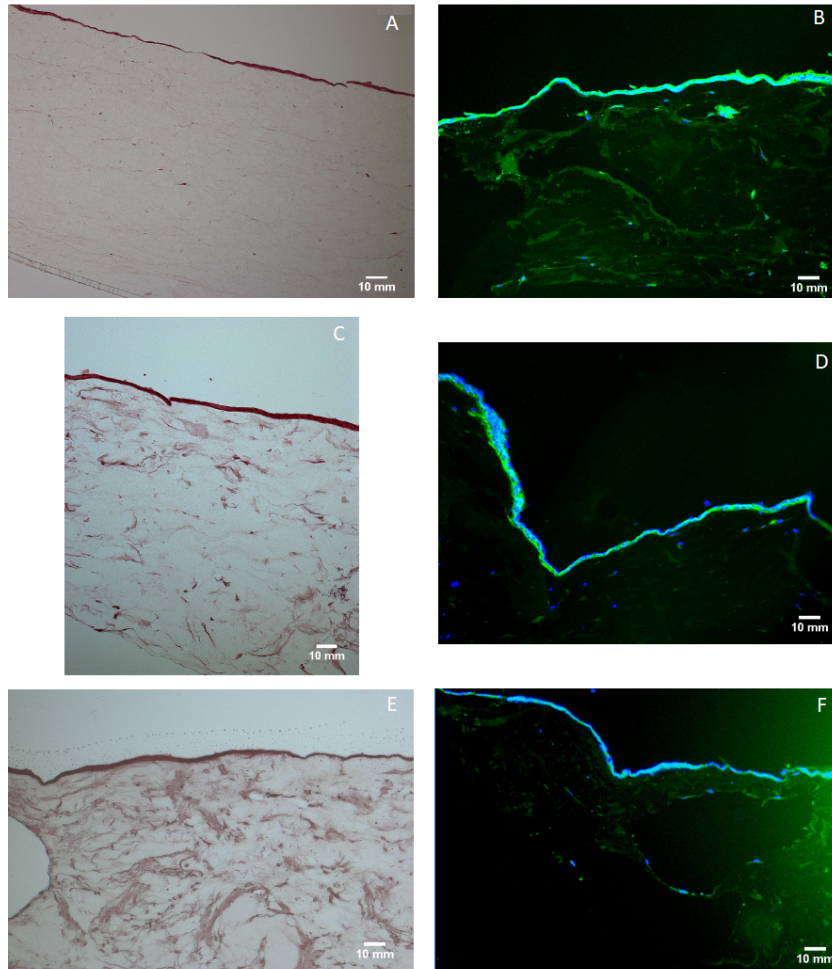
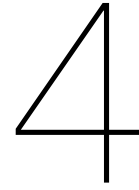


Figure 3.23: Left: Haematoxylin & Eosin Staining of psoriatic dermo-epidermal hydrogels of 5mg/mL collagen concentration – manually produced (A), 10mg/mL collagen concentration - automatically produced (C) and 15mg/mL collagen concentration - automatically produced (E). The dense red layer represents the epidermis. Right: Immunofluorescent Staining of psoriatic dermo-epidermal hydrogels of 5mg/mL collagen concentrations-manually produced (B), 10mg/mL collagen concentration - automatically produced (D) and 15mg/mL collagen concentration - automatically produced (F). B, D, F images are composite with fluorescent green colour representing cytokeratin 10, a marker for differentiated keratinocytes and fluorescent blue colour dyeing the nuclei of cells.





## Discussion & Outlook

### 4.1. Optimal Mold Design

High shrinkage and inhomogeneous thickness of skin hydrogels formed into the 12mm transwell inserts with 0.4 $\mu$ m porosity inserts, as well as inconsistency between the different hydrogels are important obstacles that not only the Pharmacogenomics Lab has faced during the manual fabrication of skin models, but which have been also recorded in literature by several research groups [13, 60]. In-mold fabrication solves the issue of shrinkage, while also defines specific dimensions and thickness for the hydrogels even if excessive volume of skin constituents is accidentally pipetted or injected, ensuring homogeneity and precision of size and shape for all fabricated hydrogels regardless of the collagen concentration.

Regarding the circular molds used so far in automated injection molding, their deficits are found in their dimensions. Firstly, their complete filling requires about five times more volume of skin mixture than what is traditionally used with the transwell inserts (though theoretically it should be only double), and this is also translated to about five times more dermal fibroblasts and a higher number of seeded keratinocytes, as well. This is a restricting factor regarding the generation of psoriatic skin models, as there is limitation in the availability of diseased cells. Besides, homogeneous seeding of keratinocytes without removing the membrane of the mold is difficult in such a width, and overlapping is a potential risk when multiple pipetting is tried. This overlapping results in an inhomogeneous epidermal layer. Finally, the diameter of 23mm prevents embedding of the whole hydrogel in a single embedding mold and hence, it should be cut in four pieces prior to the embedding process which is not only additional manual work but also an undesirable intervention to the skin layers.

These issues are solved with the new mold design, which results in triplicate of rectangular hydrogels having length of 23mm, width of 6mm and thickness of 1mm. These dimensions require three times less volume of skin constituents than the old design (both ideally and in practice), and this also means three times less dermal fibroblasts and epidermal keratinocytes per hydrogel. In this way, the issue of diseased cells availability is solved. Besides, the formed hydrogels fit the dimensions of the embedding mold and a whole triplicate can be embedded in a single embedding mold, while the 6mm width also enables in-mold seeding of keratinocytes with single directional pipetting which nicely worked in the experiments of this thesis. However, the seeding is still not standardized, and therefore probably not homogeneous, which is necessary for psoriasis research.

Another disadvantage of the initial mold was the size of membrane's pores. Though the core size of human keratinocytes ranges from 11 $\mu$ m to 50 $\mu$ m [61], the smallest of them may be squeezed and pass through the 5 $\mu$ m pores, as illustrated in Figure 3.10 and supported also by transwell migration assay. Decreasing the pore size of molds' membrane to 1 $\mu$ m minimized the number of migrating cells, while no epidermal layer was anymore formed above the membrane as histology showed.

The main remaining issue is that removing the membranes prior to biological evaluation

sometimes results in partial removal of the epidermal layer when unstable 5mg/mL collagen concentration is used, and therefore keeping the membranes on the hydrogel's surfaces during the embedding and analysing procedures is still recommended. However, it has been proven not always easy to keep the membrane on the hydrogel's surface when taking it out of the mold, and there is always a risk to peel off some keratinocytes. Regarding this problem, it was noticed that in-mold fixation of hydrogels with 4% Paraformaldehyde facilitates following processing of the samples because they harden, and it is easier to isolate them. Besides, this eliminates possibilities of contaminating or damaging the skin layers during processing, as they are already fixed when manual intervention takes place.

Also, it should be again mentioned that even the rectangular molds theoretically demand a lower volume of skin mixture than what is actually pipetted into them. Each of the three inserts of the rectangular molds is theoretically filled with 138 $\mu$ L. However, in case of manual fabrication, the evaporation taking place into the incubator throughout the curing process demands almost triple volume to be pipetted for formation of dermal gels in the molds' dimensions. A similar issue exists in case of automated injection molding. During the injection, not the whole amount of injected volume enters the mold, so injection of almost triple volume is required to ensure molds' filling. This could be also the reason that the fluorescent area detected into the inserts is slightly higher than that into the molds (as the bar graphs of Figures 3.18 and 3.19 show), though more volume is injected in case of the molds. Though a volume of 400 $\mu$ L was injected in the inserts of the rectangular mold, much less volume was actually inserted, while the whole amount of 200 $\mu$ L was inserted into the transwell inserts, and these volumes were directly related to the actual number of embedded fibroblasts into the dermal matrix. For fibroblasts density of 500cells/ $\mu$ L in the suspension, this means that hydrogels in transwell inserts have 100'000 fibroblasts and each hydrogel of the rectangular mold has about 75'000 fibroblasts. This deviation in the cell number could be eliminated if instead of 200 $\mu$ L only 150 $\mu$ L were injected into the transwell inserts but the device settings allow changes of injected volume with a step of 100 $\mu$ L. However, the aim was not to achieve exactly the same number as in case of manual pipetting into transwell inserts but to decrease the cell number compared to the bigger molds and to ensure consistency between different hydrogels, and these requirements are still fulfilled.

Therefore, despite the above mentioned drawbacks, the rectangularly-shaped mold with membrane's porosity of 1 $\mu$ m remains a very good solution. This design results in dermal hydrogels of homogeneous dimensions and thickness, as well as homogeneous cells distribution and minimum migration of keratinocytes through the membrane, regardless of the collagen concentration. Now focus should be given to the standardization of in-mold keratinocytes seeding to maximize the value of the mold, and if possible to eliminate the losses of skin constituents during injection because this is also translated to loss of cells.

## 4.2. Optimal Collagen Concentration

Traditional manual production of dermo-epidermal hydrogels employs 5mg/mL concentrated collagen as the matrix in which fibroblasts will be embedded. This concentration results in unstable hydrogels that are very difficult to be handled during paraffinization and embedding procedures. Especially when the hydrogels are taken out of the mold or the transwell insert, they may be easily deformed, and this is an essential reason to fix the hydrogels with 4% Paraformaldehyde when they are still into the mold or the transwell insert, as this will harden them and make their manipulation easier and less invading. All the other concentrations result in stable hydrogels that can be easier handled. Besides, in case of 10mg/mL, 15mg/mL and 25mg/mL collagen concentration, shrinkage is not an issue even when transwell inserts are used. As it is observed in Figures 3.12 and 3.13, these hydrogels maintain their size both into molds and transwell inserts. However, homogeneous and even thickness is ensured when the molds are used and this is also important for homogeneous seeding of keratinocytes. In case of uneven thickness, most volume of keratinocytes suspensions will be gathered in the lower spots.

Regarding fibroblasts distribution into the hydrogels, no significant difference was detected between the different conditions of collagen concentration when GFP-HDFn were used.

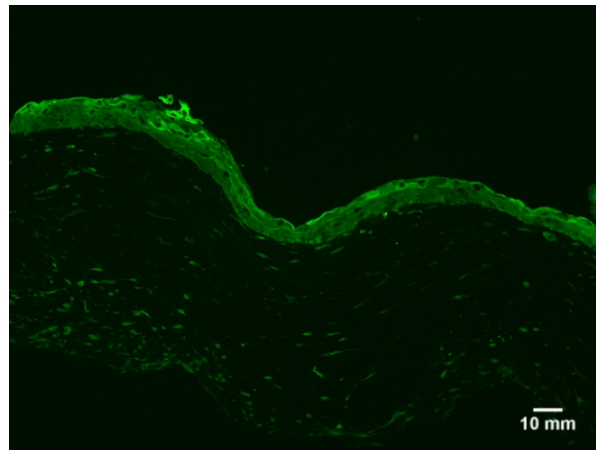


Figure 4.1: Immunofluorescent staining on dermo-epidermal hydrogel of 5mg/ml collagen concentration fabricated manually into a circular mold of 23mm diameter. High amount of cytokeratin 10 and a thick epidermal layer which represents highly differentiated keratinocytes are detected. This dermo-epidermal hydrogel was in submerged state for four days and then it was exposed to the air-liquid interface for seven more days.

Moreover, all the different collagen concentrations expressed similar keratinocytes viability and differentiation, as Haematoxylin & Eosin and immunofluorescent staining showed. The thickness of the epidermal layer did not represent significantly differentiated keratinocytes regardless of the concentration, and this has probably to do with the limited cultivation period. The dermo-epidermal hydrogels were exposed to the air-liquid interface only for five days. Elongating this period to more than seven days would have a stronger effect as the preliminary results of this collaboration have shown (Figure 4.1). Fully-differentiated epidermal layer was for example established in a published study after 14 days at the air-liquid interface <sup>[62]</sup>. However, despite the relatively thin epidermal layer, immunofluorescent staining detected cytokeratin 10, a marker for differentiated keratinocytes <sup>[63]</sup> along the whole epidermal layer, and this means that stratification had begun.

Besides, Herovici staining showed a similar pattern of collagen remodeling for all collagen concentrations apart from 5mg/mL which was not stained at all. However, this inability of Herovici staining to detect collagen fibers in low-concentrated collagen hydrogels is not translated to nonexistence of remodeling in the low-concentrated collagen and could be a limitation of the specific staining.

Therefore, the only parameter in which the effect of the different collagen concentrations actually differed was the viability of fibroblasts into the dermal hydrogels. Live-Dead staining showed that 90% of fibroblasts are alive into hydrogels of 5mg/mL collagen, while this viability decreased with the increase of the collagen concentration. Both 10mg/mL and 15mg/mL resulted in the same cell viability of about 77.5%, while 25mg/mL exhibited the lowest viability (about 60%). However, it has to be mentioned that minimum variations in viability was found between samples of 10 mg/mL and 15 mg/mL, and not in the lowest collagen concentration. For the fabrication of hydrogels of collagen concentrations higher than 5 mg/mL, automated injection molding is employed and for this reason, dermal hydrogels of 5mg/mL were also automatically fabricated in order to examine if reduced viability is directly related to increased collagen concentration or to the process of automated injection molding. However, the experiment showed that regardless of the fabrication process, viability of dermal fibroblasts in the low-concentrated hydrogels is the highest and in the same range with the negative control. Other biocompatibility studies of skin hydrogels support their hydrogels as efficient skin equivalents when cell viability was measured about 90% <sup>[64, 65]</sup>. Based on these studies, as well as the deviation from the control samples, fibroblasts viability in higher collagen concentrations is not regarded as acceptable. And considering the similar effect of the different concentrations on all the other investigated parameters (fibroblasts distribution, keratinocytes viability and differentiation), as well as the elimination of inhomogeneity and shrinkage of 5mg/mL concentrated hydrogels that molds achieve, this collagen concen-

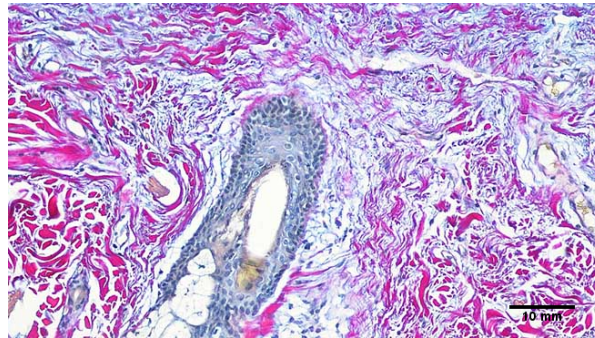


Figure 4.2: Herovici Staining on native skin depicts opalescence of reddish purple (mature collagen) and blue colour (immature collagen) [67].

tration remains the optimal one for the generation of skin models. Nevertheless, repetition of the cell viability experiments is recommended, because a higher than 5mg/mL collagen concentration could easily and fast solve several practical problems.

Regarding the remodeling of the dermal matrix in low-concentrated dermo-epidermal hydrogels, it still remains a question to be answered. Instead of staining for freshly-made collagen, immunofluorescent staining to detect extracellular proteins secreted by fibroblasts in native skin, like collagen III or fibronectin, could be implemented. This should be also applied to dermal hydrogels of higher collagen concentrations in order to more thoroughly investigate the remodeling of dermal matrix. Herovici Staining showed that in one-week old dermal hydrogels mature collagen is dominant and limited remodeling has taken place, while full remodeling occurs after 3 weeks of cultivation. This should be more deeply investigated especially when considering the theory that in Herovici Staining mature collagen (reddish purple colour) represents Collagen type I and immature collagen (blue colour) is Collagen type III [58, 66]. This theory does not conform to a full replacement of Collagen type I by Collagen type III, while it is also known that in native skin both collagen types are found (Figure 4.2). Therefore, it is recommended to also conduct immunofluorescent staining regarding different extracellular proteins for validation and reliability of this study.

### 4.3. Psoriatic Skin Model

For the fabrication of the psoriatic skin model, fibroblasts derived from patients suffering from psoriasis vulgaris were employed. All collagen concentrations, apart from 25mg/mL, were employed for the generation of the matrix in which psoriatic fibroblasts were embedded, while healthy HaCaTs were then seeded. The highest collagen concentration was excluded from this study because of the very low cell viability in them. The hydrogels were fabricated into the rectangular molds with membrane of 1 $\mu$ m pore size. Like in case of healthy dermo-epidermal hydrogels, HaCaTs were seeded four days after the fabrication of the psoriatic dermal hydrogels and three days later the gels were transferred to the air-liquid interface, in which they remained for five more days. These times were selected so that comparison with healthy skin models could take place. However, the contact between psoriatic fibroblasts and healthy HaCaTs was then restricted to only eight days in total. Most probably for this reason, the epidermal layer of the psoriatic skin model was not thicker than the epidermal layer of the healthy skin model. Saiag et al. fabricated psoriatic skin models by combining psoriatic fibroblasts and healthy keratinocytes and after nine days at the air-liquid interface they detected an epidermal outgrowth [21]. Besides, another study in which psoriatic fibroblasts and healthy keratinocytes were also combined, did not result in a thicker epidermis compared to the healthy skin model even after three weeks of exposure to the air-liquid interface [68]. The direct effect of psoriatic fibroblasts on keratinocytes proliferation is still questionable and more days in culture and especially at the state of air-liquid interface are demanded in order to derive some conclusions. Additionally, inflammatory markers that are highly expressed in psoriasis, like involucrin, or down-regulated proteins in case of this disease can be explored by immunofluorescence staining to thoroughly investigate this simplified psoriatic model [68],

while other cells types and molecules can be gradually added to look into their effect.

#### 4.4. Comparison between Automated Injection Molding and Manual Fabrication

Based on this research findings, the main advantage of the automated injection molding has to do with the use of molds for the development of the skin models. The molds define and preserve specific dimensions of the hydrogels, prevent self-contraction and achieve within and between hydrogels homogeneity. Also, automated injection molding prevails over manual fabrication as it is a standardized fabrication method, limiting the human factor regarding the stirring of the skin constituents and their insertion into the culture inserts (molds or transwell inserts). Besides, it allows the generation of more stable and easily processed samples via the employment of collagen concentrations higher than 5mg/mL, which are more viscous and hence they cannot be pipetted.

However, 5mg/mL was proved to be the optimal collagen concentration thanks to the best fibroblasts' response despite its instability and difficult manipulation. And due to the high time demands for sterilizing the device and its individual components as well as for loading of skin constituents into the cartridge, simple manual pipetting of skin constituents remains easier and faster for the development of dermal models. Besides, as long as the seeding of keratinocytes is conducted manually, biologists regard as time-consuming the preparation of the device just for the generation of the dermal component that they can be quickly manually produce. Moreover, molds can be utilized also in the manual fabrication, as this research showed, and hence an important benefit of the automated injection molding can be still deployed.

However, the next generation of the device in which seeding of keratinocytes is also automated has been built and is currently being examined in the generation of consistent dermo-epidermal models. This would be important progress as in-mold manual seeding of keratinocytes is strongly dependent on researcher experience and it is difficult to achieve consistency, while it would also boost again the value of the device, even if it is still slower than manual production, as now a full dermo-epidermal model could be formed in a standardized way. As long as manual seeding of keratinocytes is conducted, it may be beneficial to remove the upper membrane of the mold prior to keratinocytes seeding so that presence or detachment of the membrane does not affect the epidermal layer. This might be difficult in case of unstable 5mg/mL collagen concentration hydrogels, but it should be attempted as it would facilitate the manual seeding of keratinocytes, which would be an improved version of the seeding in transwell inserts due to the equal thickness and the even surface of the in-mold hydrogels.

Also, though the several advantages of the new mold design developed in this project, the next generation of molds should be also designed if pharmaceutical screening is taken into consideration. Screening is usually implemented 96-well plates, the wells of which have 6mm diameter. Therefore, molds in this size should be designed so that formed hydrogels can be later transferred to a 96-well plate for conduction of drug screening, or even better would be the development of a well-plate analogue consisting of 96 small circular molds instead of wells so that screening could be directly implemented in this, eliminating the manual work of removing the gels and placing them into a classic 96-well plate. In this case, the value of the injection molding device is further enhanced regardless of the employed collagen concentration as manual pipetting can be not only inconsistent but also really laborious in case of large scale studies.

All the above issues should be taken into account when developing the next generation of the device. For example, the currently used mixing nozzle has a diameter of 5mm, and a smaller one should be certainly used to allow injection in such a small mold. Also, the fabrication of such a mold can be tedious and hence, when its design is finalized, and its use is established, it would be possibly worthy to assign the whole building and sterilization of the new mold to a specialized company. Besides, one more improvement would be to decrease the step size that the injected volume changes to achieve better precision and offer more options to the researchers. Also, slight vibrations of the cartridge walls could be

actuated for continuous stirring of cell suspension to ensure equal deposition of cells into the different hydrogels. Last but not least, for the generation of psoriatic skin models it should be considered that several cell types must be combined in the dermal matrix; dermal fibroblasts, vascular endothelial cells and lymphocytes. Therefore, the device should automatically blend the dermal matrix with all these different cell types and later seed the keratinocytes on top to fully automate the fabrication process. For this purpose, probably several chambers leaching into a single mixing nozzle or syringe should be incorporated.

# 5

## Conclusions

Throughout the conduction of this master thesis, the automated injection molding of dermo-epidermal models was examined compared to the manual pipetting of these models. Automated injection molding produces dermo-epidermal hydrogels of similar biological performance with the manually fabricated ones in a more standardized way, but the high collagen concentration traditionally employed in this process is toxic for the fibroblasts and hence, lower collagen concentrations must be used. A dermal matrix of 5mg/mL collagen concentration was found to achieve the highest fibroblasts viability and considering that it is the only concentration that can be both manually and automatically treated, it questions the need for the device in its current state. This results from the time needed for sterilizing and assembling all the components used in this process, which exceeds the time required for the manual pipetting of the dermal constituents. However, automated injection molding is more standardized compared to manual production thanks not only to the utilization of molds that define and preserve hydrogels' dimensions but also to the automatic mixing and injection of the skin constituents which is standardized and independent of manual pipetting precision.

The use of molds solves issues of shrinkage and inhomogeneity that are usually observed when hydrogels are formed into transwell inserts. A simple but effective solution regarding the instability of the low collagen concentrated (i.e. 5mg/mL) hydrogels during processing was found, facilitating their manipulation and biological evaluation. Therefore, even if manual fabrication is chosen, molds can be still utilized to achieve consistency and homogeneity within and between dermo-epidermal models.

The final objective of this research was to generate a first psoriatic model including psoriatic fibroblasts and healthy keratinocytes. The preliminary results showed a slightly differentiated epidermal layer very similar with the one in healthy dermo-epidermal models, probably because of the limited cultivation period of the skin models.

The next steps of this collaboration project should include the evaluation of the automated seeding of keratinocytes in hydrogels formed into the new mold as well as the elongation of the cultivation period for this first simple psoriatic model.



# Bibliography

- [1] K. Hoehn, E. N. Marieb, Study Guide Human Anatomy & Physiology, Ninth Edition, Pearson, Boston, MA, 2013.
- [2] S. Vijayavenkataraman, W. F. Lu, J. Y. H. Fuh, Biofabrication 2016, 8, 032001.
- [3] L. L. & OpenStax, "Anatomy and Physiology I," can be found under <https://courses.lumenlearning.com/ap1/chapter/layers-of-the-skin/>, n.d.
- [4] S. Guerrero-Aspizua, C. J. Conti, E. Zapatero-Solana, F. Larcher, M. D. Ro, Translating Regenerative Medicine to the Clinic 2016, 107.
- [5] S. Bttcher-Haberzeth, T. Biedermann, E. Reichmann, Burns 2010, 36, 450.
- [6] D. J. Geer, D. D. Swartz, S. T. Andreadis, Tissue Engineering 2002, 8, 787.
- [7] F. Pati, J. Jang, J. W. Lee, D.-W. Cho, Essentials of 3D Biofabrication and Translation 2015, 123.
- [8] Y. Jin, H. Bi, Burns & Trauma 2013, 1, 63.
- [9] Psoriasis-Overview, can be found under <https://www.dermaharmony.com/Psoriasis/>, n.d.
- [10] K. Guthrie, A. Bruce, N. Sangha, E. Rivera, J. Basu, Trends in Biotechnology 2013, 31, 505.
- [11] G. Lu, S. Huang, International Wound Journal 2012, 10, 365.
- [12] A. D. Metcalfe, M. W. Ferguson, Biomaterials 2007, 28, 5100.
- [13] E. Braziulis, M. Diezi, T. Biedermann, L. Pontiggia, M. Schmucki, F. Hartmann-Fritsch, J. Luginbhl, C. Schiestl, M. Meuli, E. Reichmann, Tissue Engineering Part C: Methods 2012, 18, 464.
- [14] E. Blozik, M. Scherer, Diabetes Care 2007, 31, 693.
- [15] Beacon Projects can be found under <https://www.lifesciences.fraunhofer.de/en/leuchtturmprojekte/gesch2/hautfabrik.html#tabpanel-3>.
- [16] S. Macneil, Nature 2007, 445, 874.
- [17] L. Semlin, M. Schfer-Korting, C. Borelli, H. C. Korting, Drug Discovery Today 2011, 16, 132.
- [18] K. R. Feingold, "Kenneth R. Feingold," can be found under <http://www.jlr.org/content/53/8/1427>, 2012.
- [19] E. Higgins, Medicine 2017, 45, 368.
- [20] C. Quan, M. K. Cho, Y. Shao, L. E. Miannecki, E. Liao, D. Perry, T. Quan, Protein & Cell 2015, 6, 890.
- [21] P. Saiag, B. Coulomb, C. Lebreton, E. Bell, L. Dubertret, Science 1985, 230, 669.
- [22] A. Wojas-Pelc, M. Ciszek, M. Kurnyta, J. Marcinkiewicz. Central European Journal of Immunology 2007, 31(3), 3-4.

- [23] A. Pietrzak, A. Zalewska, G. Chodorowska, P. Nockowski, A. Michalak-Stoma, P. Osem-lak, D. Krasowska, *Folia Histochemica et Cytobiologica* 2008, 46, DOI 10.2478/v10042-008-0002-y.
- [24] K. Adsad, PhD Thesis, University of Bradford, 2010
- [25] "Psoriasis-Overview," can be found under <https://www.dermaharmony.com/Psoriasis/>, n.d.
- [26] M. Garcia, M. J. Escamez, M. Carretero, I. Mirones, L. Martinez-Santamaria, M. Navarro, J. L. Jorcano, A. Meana, M. D. Rio, F. Larcher, *Molecular Carcinogenesis* 2007, 46, 741.
- [27] N. Cubo, M. Garcia, J. F. D. Caizo, D. Velasco, J. L. Jorcano, *Biofabrication* 2016, 9, 015006.
- [28] D. M. Danilenko, *Veterinary Pathology* 2008, 45, 563.
- [29] S. Guerrero-Aspizua, M. Garca, R. Murillas, L. Retamosa, N. Illera, B. Duarte, A. Holgun, S. Puig, M. I. Hernandez, A. Meana, J. L. Jorcano, F. Larcher, M. Carretero, M. D. Ro, *The American Journal of Pathology* 2010, 177, 3112.
- [30] A. Chiricozzi, M. Romanelli, S. Panduri, E. Donetti, F. Prignano, *Histology and Histopathology* 2017, 32.
- [31] B. Roy, M. Simard, I. Lorthois, A. Blanger, M. Maheux, A. Duque-Fernandez, G. Rioux, P. Simard, M. Deslauriers, L.-C. Masson, A. Morin, R. Pouliot, *Skin Tissue Models for Regenerative Medicine* 2018, 103.
- [32] J. Jean, M. Lapointe, J. Soucy, R. Pouliot, *Journal of Dermatological Science* 2009, 53, 19.
- [33] News, can be found under <http://reconstructed-humanepidermis.com/>, n.d.
- [34] C. Asbill, N. Kim, A. El-Kattan, K. Creek, P. Wertz, B. Michniak, *Pharmaceutical Research* 2000, 17, 10921097
- [35] D. A. Medalie, S. A. Eming, R. G. Tompkins, M. L. Yarmush, G. G. Krueger, J. R. Morgan, *Journal of Investigative Dermatology* 1996, 107, 121.13
- [36] M. H. Mohammadi, B. H. Araghi, V. Beydaghi, A. Geraili, F. Moradi, P. Jafari, M. Jan-maleki, K. P. Valente, M. Akbari, A. Sanati-Nezhad, *Advanced Healthcare Materials* 2016, 5, 2454.
- [37] G. Sriram, M. Alberti, Y. Dancik, B. Wu, R. Wu, Z. Feng, S. Ramasamy, P. L. Bigliardi, M. Bigliardi-Qi, Z. Wang, *Materials Today* 2018, 21, 326.
- [38] M. Wufuer, G. Lee, W. Hur, B. Jeon, B. J. Kim, T. H. Choi, S. Lee, *Scientific Reports* 2016, 6, DOI 10.1038/srep37471.
- [39] S. Park, K. Park, *Polymers* 2016, 8, 23.
- [40] L. Pontiggia, A. Klar, S. Bttcher-Haberzeth, T. Biedermann, M. Meuli, E. Reichmann, *Pediatric Surgery International* 2013, 29, 249.
- [41] Manual Pipetting Risks - Labtimes, can be found under <http://www.labtimes.org/labtimes/issues/lt2010/lt04/lt2010045459.pdf>.
- [42] The skin factory, can be found under <https://www.soci.org/Chemistry-and-Industry/CnIData/2011/18/The-skin-factory.aspx>, n.d.
- [43] V. Lee, G. Singh, J. P. Trasatti, C. Bjornsson, X. Xu, T. N. Tran, S.-S. Yoo, G. Dai, P. Karande, *Tissue Engineering Part C:Methods* 2014, 20, 473.

- [44] F. F. Schmid, T. Schwarz, M. Klos, W. Schuberthan, H. Walles, J. Hansmann, F. K. Groeber, *Applied In Vitro Toxicology* 2016, 2, 118.
- [45] Y. R. Park, H. W. Ju, J. M. Lee, D.-K. Kim, O. J. Lee, B. M. Moon, H. J. Park, J. Y. Jeong, Y. K. Yeon, C. H. Park, *International Journal of Biological Macromolecules* 2016, 93, 1567.
- [46] I. T. Ozbolat, M. Hospodiuk, *Biomaterials* 2016, 76, 321.
- [47] D. G. Nguyen, S. L. Pentoney, *Drug Discovery Today: Technologies* 2017, 23, 37.
- [48] X. Cui, T. Boland, D. D. dlima, M. K. Lotz, *Recent Patents on Drug Delivery & Formulation* 2012, 6, 149.
- [49] S. C. Fox, T. Biedermann, M. Schmid Daners, E. Reichmann, M. Meboldt, *Personalised Therapies for Regenerative Medicine TERMIS-EU 2017 Conference*, Davos, Switzerland 2017.
- [50] S. C. Fox, T. Biedermann, J. Polak, J. Hu, M. Schmid Daners, E. Reichmann, M. Meboldt, *International Conference of Biofabrication*, Beijing, China 2017.
- [51] J. Hu, *Patch Forming of Bioengineered Skin, Development and Validation of a Functional Prototype for Automation*, Master thesis 2017.
- [52] M. Sarkiri, *Expansion of dermal patch-forming device for the automated production of full dermo-epidermal equivalents*, Research internship report 2017.
- [53] F. V. Ruissen, G. J. D. Jongh, P. L. Zeeuwen, P. E. V. Erp, P. Madsen, J. Schalkwijk, *Journal of Cellular Physiology* 1996, 168, 442.
- [54] "Inflammation," can be found under <http://www.epistem.co.uk/inflammation/psoriasis.php>, n.d.
- [55] J. Jean, M. Lapointe, J. Soucy, R. Pouliot, *Journal of Dermatological Science* 2009, 53, 19.
- [56] A. Michalak-Stoma, P. Nockowski, P. Osemlak, T. Paszkowski, J. M. Roliński, *Clinica Chimica Acta* 2008, 394, 7.
- [57] J. Meephansan, U. Subpayasarn, M. Komine, M. Ohtsuki, *An Interdisciplinary Approach to Psoriasis* 2017, DOI 10.5772/intechopen.68421.
- [58] K. Adsad, PhD Thesis, University of Bradford, 2010
- [59] J. Polak, *Biological Study of Bioengineered Skin, Investigation of Injection Molded Bi-layered Skin Equivalents and Suitable Biomaterials*, Master thesis 2018.
- [60] A. El-Fiqi, J. H. Lee, E.-J. Lee, H.-W. Kim, *Acta Biomaterialia* 2013, 9, 9508.
- [61] Y. Barrandon, H. Green, *Proceedings of the National Academy of Sciences* 1985, 82, 5390.
- [62] M. Rosdy, L.-C. Clauss, *Journal of Investigative Dermatology* 1990, 95, 409.
- [63] can be found under <http://www.antibodybeyond.com/reviews/cell-markers/keratinocyte-marker.htm>, n.d.
- [64] D. Chejara, M. Mabrouk, P. Kumar, Y. Choonara, P. Kondiah, R. Badhe, L. Toit, D. Bijukumar, V. Pillay, *Marine Drugs* 2017, 15, 257.
- [65] H. Sun, J. Zhou, Z. Huang, L. Qu, N. Lin, C. Liang, R. Dai, L. Tang, F. Tian, *International Journal of Nanomedicine* 2017, Volume 12, 3109.
- [66] A. Fitzgerald, J. Kirkpatrick, I. Foo, I. Naylor, *Burns* 1996, 22, 200.

- 
- [67] "Histologie et immunohistochimie," can be found under <https://www.bioalternatives.com/histologie-immunohistologie-immunohistofluorescence/>, n.d.
- [68] J. Jean, M. Lapointe, J. Soucy, R. Pouliot, *Journal of Dermatological Science* 2009, 53, 19.